



The multistep oxidation of cholesterol to pregnenolone by human cytochrome P450 11A1 is highly processive

Received for publication, September 18, 2023, and in revised form, November 17, 2023 Published, Papers in Press, November 24, 2023, <https://doi.org/10.1016/j.jbc.2023.105495>

Kevin D. McCarty[†], Lu Liu[†], Yasuhiro Tateishi[†], Hannah L. Wapshott-Stehli[†], and F. Peter Guengerich*

From the Department of Biochemistry, Vanderbilt University School of Medicine, Nashville, Tennessee, USA

Reviewed by members of the JBC Editorial Board. Edited by Joseph Jez

Cytochrome P450 (P450, CYP) 11A1 is the classical cholesterol side chain cleavage enzyme (P450_{scc}) that removes six carbons of the side chain, the first and rate-limiting step in the synthesis of all mammalian steroids. The reaction is a 3-step, 6-electron oxidation that proceeds *via* formation of 22R-hydroxy (OH) and 20R,22R-(OH)₂ cholesterol, yielding pregnenolone. We expressed human P450 11A1 in bacteria, purified the enzyme in the absence of nonionic detergents, and assayed pregnenolone formation by HPLC-mass spectrometry of the dansyl hydrazone. The reaction was inhibited by the nonionic detergent Tween 20, and several lipids did not enhance enzymatic activity. The 22R-OH and 20R,22R-(OH)₂ cholesterol intermediates were bound to P450 11A1 relatively tightly, as judged by steady-state optical titrations and *k*_{off} rates. The electron donor adrenodoxin had little effect on binding; the substrate cholesterol showed a ~5-fold stimulatory effect on the binding of adrenodoxin to P450 11A1. Presteady-state single-turnover kinetic analysis was consistent with a highly processive reaction with rates of intermediate oxidation steps far exceeding dissociation rates for products and substrates. The presteady-state kinetic analysis revealed a second di-OH cholesterol product, separable by HPLC, in addition to 20R,22R-(OH)₂ cholesterol, which we characterized as a rotamer that was also converted to pregnenolone at a similar rate. The first oxidation step (at C-22) is the slowest, limiting the overall rate of cleavage. *d*₃-Cholesterol showed no kinetic deuterium isotope effect on C-22, indicating that C-H bond cleavage is not rate-limiting in the first hydroxylation step.

The synthesis of all steroids proceeds from the cleavage of the 6-carbon tail from cholesterol by cytochrome P450 (P450, CYP) 11A1, the “side-chain cleavage” enzyme (P450_{scc}) (Fig. 1). This mitochondrial enzyme, localized in adrenals and other hormone-producing organs, is highly regulated, and genetic variations can cause congenital adrenal insufficiency (1). Even though this enzyme has a well-defined function in steroid biosynthesis, it also catalyzes reactions with other substrates, including 7-dehydrocholesterol, other steroids (2, 3), vitamin D₃ (4), and even some drugs (5).

Successful catalysis of P450 11A1 reactions requires reducing equivalents delivered by the mitochondrial P450 redox partners, adrenodoxin (Adx) and adrenodoxin reductase (AdR). Electrons (derived from NADPH) are shuttled through the flavin domains of the membrane-bound AdR protein to the soluble iron-sulfur matrix protein Adx. Electrons are subsequently delivered to P450 11A1 by Adx, thus facilitating the activation of molecular oxygen by P450.

X-ray crystal structures of P450 11A1 have been published (6, 7). All three steps of the reaction (Fig. 1) are considered to involve the high valent oxygen species known as compound I (FeO³⁺), based on cryoreduction/annealing data which demonstrated the catalytic competence of artificially formed Compound I (8, 9). Further details of the unusual oxidative cleavage of the 20R,22R-(OH)₂ sterol by P450 11A1—that is, nucleophilic attack of a C-20 or C-22 hydroxyl group on Compound I—been provided through ¹⁸O-labeling studies (10), although an alternate explanation of the results has also been presented, based on theoretical calculations (11).

P450 11A1 has been studied for many years, with much of the early work involving the enzyme isolated from bovine adrenals. The isolation procedures vary, and many include the use of nonionic detergents, with the recombinant human enzyme as well as bovine P450 11A1. The assays that have been used for measuring enzyme activity (formation of pregnenolone) also vary considerably, including radioimmunoassay (12, 13), radio-TLC (14), gas chromatography (of derivatives) (15), and radio-HPLC (16). Not surprisingly, then, the reported activities of the purified bovine and human enzymes are quite variable in these assays, ranging from 0.29 to 34 nmol pregnenolone formed min⁻¹ (nmol P450)⁻¹ (12, 16–21).

An important question, which we now address, is how processive the overall 3-step reaction is, that is, how likely each product is to dissociate from the enzyme before acting as a substrate for the next oxidation step. Early work on the enzyme has been reviewed by Lieberman and Lin (22). No hydroxy (OH) intermediates (between cholesterol and pregnenolone) were found in some cases (14, 16) but were seen in other steady-state studies, at low levels (15, 23), or in a reaction in which the enzyme was artificially cycled (24). Sugano *et al.* (21) reported that the intermediate 20R,22R-(OH)₂ cholesterol could be detected as an intermediate when 22R-OH cholesterol was incubated with P450 11A1 but only when relatively

[†] These authors should be considered cofirst authors.

* For correspondence: F. Peter Guengerich, f.guengerich@vanderbilt.edu.

Processivity of P450 11A1

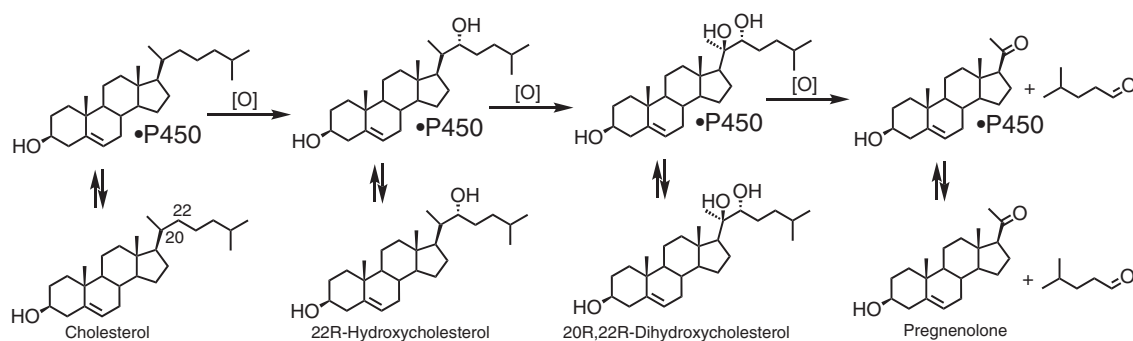


Figure 1. The three-step oxidation of cholesterol to pregnenolone catalyzed by P450 11A1. The equilibria between free and enzyme-bound steroids are shown and are the subject of this investigation.

low concentrations of Adx (*i.e.*, equimolar) were used. The authors interpreted the result as indicating that the binding of 20R,22R-(OH)₂ cholesterol was weaker when lower concentrations of this accessory protein Adx were used. Tuckey and Cameron (25) were also able to convert 22R-OH cholesterol to 20R,22R-(OH)₂ in human placental mitochondria. Lambeth *et al.* (12) concluded that each oxidation step occurs at approximately the same rate at 37 °C.

Although the synthetic steroid intermediates in the reaction pathway (Fig. 1) have been available for several years, the binding of all of these to P450 11A1 has not been investigated rigorously, in our opinion. Orme-Johnson *et al.* (26) reported K_d values of 4.9 and 81 nM for the bovine P450 11A1 complexes with 22R-OH cholesterol and 20R,22R-(OH)₂ cholesterol, values obtained using equilibrium dialysis. Jefcoate reported a K_d of 0.40 to 0.45 μ M for 20R,22R-(OH)₂ cholesterol with the rat enzyme (27). Lambeth *et al.* (12) also considered the binding of the hydroxycholesterols, expressing K_d values in the context of a sterol to phosphatidylcholine ratio. Adx was reported to strongly enhance binding. The authors indicated that the rates of both binding and dissociation of 20R,22R-(OH)₂ cholesterol with bovine P450 11A1 were >300 s⁻¹ (based on attempts to use stopped-flow kinetics). They also concluded, based on the spectral sterol/phospholipid ratio data, that the "...intermediates are bound 2 to 3 orders of magnitude more tightly than cholesterol," although even with a typical k_{on} rate of 10^6 M⁻¹ s⁻¹ (28, 29) and a k_{off} rate of 300 s⁻¹ would only correspond to a K_d of 300 μ M (and k_{on} rate of 10^7 M⁻¹ s⁻¹ to a K_d value of 30 μ M).

The availability of recombinant human P450 11A1, its accessory proteins Adx and AdR and the intermediates in the reaction pathway (Fig. 1; Figs. S1–S8) allowed for the systematic investigation of the kinetic processivity of P450 11A1, using features of a general approach that we have applied with other multistep P450s (30–32), most recently with human P450 51A1 (33). We have also used a detergent-free preparation of the recombinant human enzyme to address questions about the contributions of lipids (and detergents) and the role of the accessory protein Adx in binding ligands, as well as C–H bonding breaking as a rate-limiting step. A kinetic model for the reaction was developed based on the results. We also report the formation and cleavage of a second conformer of 20R,22R-(OH)₂ cholesterol in the normal

reaction, as revealed by rapid-quench kinetics and HPLC separation.

Results

Expression, purification, and assays

We had expressed and purified human P450 11A1 previously, with the use of the nonionic detergent pentaethylene glycol monoethyl ether (C8E5) (3). We experienced low expression yields for P450 11A1 and used a different vector (pET23C+) for this study, using the same amino acid sequence as before (Fig. S9). The new vector notably employs a T7 promoter (Fig. S10) which recruits the T7 RNA polymerase for faster and more efficient transcription. Typical yields of P450 11A1 were 150 nmol purified enzyme (liter culture)⁻¹.

Nonionic detergents are inherently difficult to remove from P450 enzymes (34). Accordingly, we had concerns about the presence of any residual nonionic detergent in the preparation, which might interfere in a careful study of the interactions of the enzyme with substrates. Although most of the P450 11A1 literature protocols utilize nonionic detergents, (mainly Tween 20) in purification (and even in assays), our preliminary assays showed that Tween 20 was inhibitory. However, we also noted that attempts to remove Tween 20 from preparations (*e.g.*, polystyrene beads, adsorption to hydroxylapatite and other chromatography columns followed by washing and elution) resulted in (i) enzyme precipitation or (ii) incomplete removal of the Tween 20 (as assayed colorimetrically (35)). Even under the best conditions, P450 11A1 preparations still contained ~ 2 mg Tween 20 (nmol P450)⁻¹.

We developed a procedure (suggested by Prof. Donghak Kim and Changmin Kim, Konkuk University, Seoul) in which the cell membranes were lysed in the presence of the ionic detergent CHAPS and applied to an Ni²⁺-nitrilo triacetate affinity column. After washing to remove CHAPS, the protein (electrophoretically homogeneous, Figs. S11 and S12) could be eluted with a high imidazole concentration and remained soluble.

The substrate cholesterol and its 22R-OH and 20R,22R-(OH)₂ products were delivered in 2-hydroxypropyl- β -cyclodextrin (HPCD) (36) in assays, circumventing the need to use any detergents or organic solvents. P450 11A1 readily coupled with the electron carrier Adx, a soluble protein, and the

concentration of Adx was optimized (Fig. 2) (37). Tween 20 was found to be inhibitory at all concentrations $>0.008\%$ (w/v), under these conditions (Fig. 3). When P450 11A1 was solubilized with CHAPS and purified, the rate of the conversion of cholesterol to pregnenolone was routinely ~ 5 to 8 min^{-1} (i.e., nmol pregnenolone formed min^{-1} (nmol P450) $^{-1}$), which is as high or higher than many (but not all (20)) previous values. Further, the activity was not enhanced by the addition of L- α -dilauroyl-*sn*-glycero-3-phosphocholine or L- α -dioleoyl-*sn*-glycero-3-phosphocholine and was inhibited by a combination of L- α -dioleoyl-*sn*-glycero-3-phosphocholine and cardiolipin (Fig. 4), in contrast to literature on the bovine enzyme (12, 38–40).

Accordingly, all steady-state assays were done, unless otherwise noted, with a P450 11A1:Adx:AdR molar ratio of 1:40:2 (Fig. 2, that is, $0.25 \mu\text{M}$ P450, $10 \mu\text{M}$ Adx, and $0.5 \mu\text{M}$ AdR), in the absence of added lipid or detergent, and with the addition of sterol substrates in HPCD (stock 45% w/v).

As mentioned in the Introduction, many types of assays have been used to monitor the steady-state conversion of cholesterol to pregnenolone (12, 14–21). A reliable and sensitive method was required that could be used for presteady-state reactions and was not reliant on the presence of isotope in cholesterol, in that, we also worked with 22R-OH cholesterol and 20R,22R-(OH) $_2$ cholesterol as substrates. We utilized a method based on our work with P450 17A1 (41, 42), in which we derivatized the product pregnenolone as its dansyl hydrazone and separated it by ultra-performance liquid chromatography (UPLC) with detection by positive ion electrospray mass spectrometry (MS). The steroid dehydroepiandrosterone (DHEA) was used as an internal standard.

Steady-state kinetics

The dansyl derivatization method provided a sensitive means by which one can monitor the formation of pregnenolone in steady-state assays (Fig. 5). The kinetic analyses showed that the oxidations of cholesterol and its intermediates (22R-OH and 20R,22R-(OH) $_2$ cholesterol) were similar in both

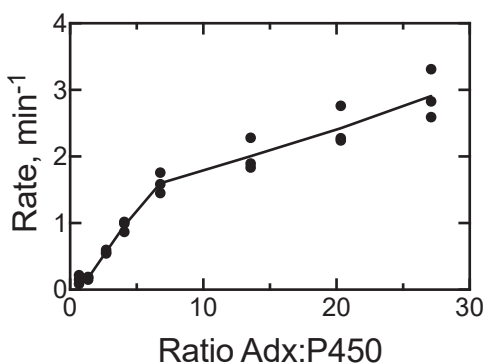


Figure 2. Dependence of catalytic activity on Adx concentration. Incubations (5 min, 37 °C) were run with $0.25 \mu\text{M}$ P450 11A1 ($0.5 \mu\text{M}$ AdR), $50 \mu\text{M}$ cholesterol, and a variable concentration (0.17 – $6.8 \mu\text{M}$) of Adx and were initiated with an NADPH generating system (Experimental procedures). Reactions were run in triplicate and the conversion of cholesterol to pregnenolone was calculated and plotted (nmol pregnenolone formed min^{-1} (nmol P450) $^{-1}$). AdR, adrenodoxin reductase; Adx, adrenodoxin; P450, cytochrome P450.

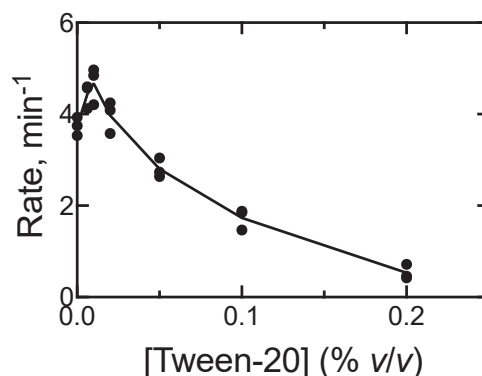


Figure 3. Effect of Tween 20 on P450 11A1 catalytic activity. Incubations (5 min, 37 °C) were run with $0.25 \mu\text{M}$ P450 11A1 ($0.5 \mu\text{M}$ AdR) and $50 \mu\text{M}$ cholesterol with an excess (40-fold) of Adx and were initiated with an NADPH generating system (Experimental procedures). Reactions were run in triplicate and the conversion of cholesterol to pregnenolone was calculated and plotted (nmol pregnenolone formed min^{-1} (nmol P450) $^{-1}$). (Note: These assays were done with P450 11A1 purified in the absence of Tween 20.). AdR, adrenodoxin reductase; Adx, adrenodoxin; P450, cytochrome P450.

k_{cat} and k_{cat}/K_m , with the 20R,22R-(OH) $_2$ sterol being ~ 2 -fold greater in both parameters relative to the starting substrate. Interestingly, while 20R,22S-(OH) $_2$ cholesterol—a nonnative substrate—was nearly 3-fold lower in k_{cat} than the native diol, it was roughly equal in k_{cat}/K_m indicating that it is oxidized almost as efficiently as the native substrate (Table 1). P450

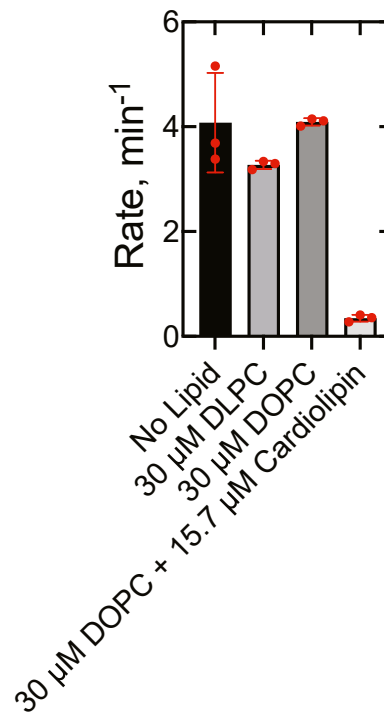


Figure 4. Effects of lipids on P450 11A1 activity. Incubations (5 min, 37 °C) were run with $30 \mu\text{M}$ phospholipid, $0.25 \mu\text{M}$ P450 11A1 ($0.5 \mu\text{M}$ AdR), and $50 \mu\text{M}$ cholesterol with an excess (40-fold) of Adx and were initiated with an NADPH generating system (Experimental procedures). Reactions were run in triplicate and the conversion of cholesterol to pregnenolone was calculated and plotted (nmol pregnenolone formed min^{-1} (nmol P450) $^{-1}$). AdR, adrenodoxin reductase; Adx, adrenodoxin; P450, cytochrome P450.

Processivity of P450 11A1

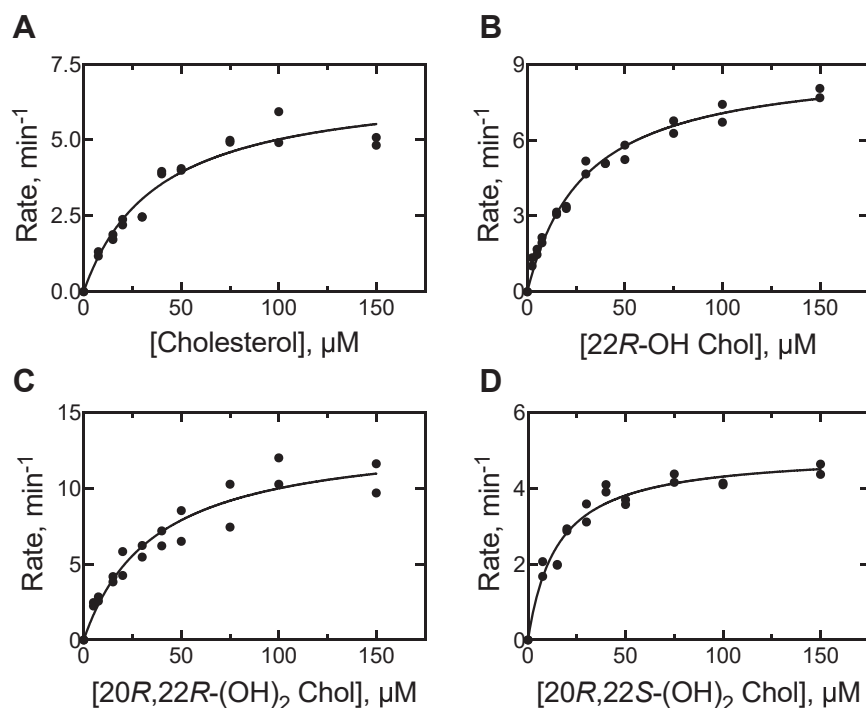


Figure 5. Steady-state kinetics of oxidation of cholesterol, 22R-hydroxycholesterol, 20R,22R-dihydroxycholesterol, and 20R,22S-dihydroxycholesterol to pregnenolone by P450 11A1. The individual substrates were incubated with the reconstituted P450 11A1 system (0.25 μM P450, 0.5 μM AdR, and 10 μM Adx), initiated with an NADPH generating system (Experimental procedures), and the product pregnenolone was extracted, derivatized, and quantified by UPLC-MS. Chol: cholesterol. **A**, cholesterol: k_{cat} $6.9 \pm 0.5 \text{ min}^{-1}$, K_m $38 \pm 6 \mu\text{M}$, k_{cat}/K_m $0.18 \pm 0.03 \mu\text{M}^{-1} \text{ min}^{-1}$. **B**, 22R-OH cholesterol: k_{cat} $9.1 \pm 0.3 \text{ min}^{-1}$, K_m $29 \pm 3 \mu\text{M}$, k_{cat}/K_m $0.31 \pm 0.03 \mu\text{M}^{-1} \text{ min}^{-1}$. **C**, 20R,22R-(OH)₂ cholesterol: k_{cat} $14 \pm 1 \text{ min}^{-1}$, K_m $36 \pm 7 \mu\text{M}$, k_{cat}/K_m $0.38 \pm 0.07 \mu\text{M}^{-1} \text{ min}^{-1}$. **D**, 20R,22S-(OH)₂ cholesterol: k_{cat} $5.0 \pm 0.2 \text{ min}^{-1}$, K_m $15 \pm 2 \mu\text{M}$, k_{cat}/K_m $0.33 \pm 0.05 \mu\text{M}^{-1} \text{ min}^{-1}$. See Table 1. Rates are presented on the y-axis as nmol product (pregnenolone) formed min^{-1} (nmol P450)⁻¹. Incubations were run in duplicate and the conversion of sterol to pregnenolone was calculated and plotted. The nonlinear regression fits include the Prism error estimates for internal fitting (SE). The estimated parameters were not corrected using a quadratic equation, due to high K_m values relative to enzyme concentration. AdR, adrenodoxin reductase; P450, cytochrome P450; UPLC, ultra-performance liquid chromatography.

11A1 also oxidized [1,2-³H] cholesterol at a similar rate to that which we report using the dansyl derivatization method (Fig. S13), giving us further confidence in the accuracy of our LC-MS based approach.

Steady-state binding of steroids to P450 11A1

Ligand binding constants were determined from the low-to-high-spin (hypsochromic) spectral transition that occurs at the P450 heme as substrate entering the active site replaces water as the sixth axial heme ligand. This so-called “Type I” shift (43) was observed in the binding of each of the studied sterols to P450 11A1 (Fig. 6). Binding titrations were performed in a 10-cm cell with low concentrations (0.1 μM) of P450 due to our estimation of low K_d values in preliminary experiments.

The K_d values calculated for all sterols were sub- μM (when quadratic fitting was applied) but were notably below the enzyme concentration for the oxidation intermediates (22R-OH and 20R,22R-(OH)₂), indicating that these measurements likely contain error. As a result, we subsequently measured k_{off} values of the P450-sterol complexes, which were consistent with the low K_d values observed (see below). Binding titrations were repeated in the presence of Adx (1 M equivalent, Fig. 6), although no significant effect was observed, even when Adx was added in excess (10-fold with cholesterol as the substrate, data not shown). The enzymatic byproduct of cholesterol side chain cleavage (4-methylpentanal) did not induce a spectral shift with P450 11A1, even at comparably high (up to 1 mM) concentrations.

Table 1
Oxidation and binding kinetic parameters of cholesterol and intermediates with P450 11A1

Steroid	K_d , μM		k_{cat} , s^{-1}	K_m , μM	k_{cat}/K_m , $\text{M}^{-1} \text{s}^{-1}$	k_{off} , s^{-1}
	(-) Adx	(+) Adx				
Cholesterol	0.12 ± 0.01	0.11 ± 0.01	0.12 ± 0.01	38 ± 6	$3.2 \pm 0.5 \times 10^3$	0.24 ± 0.01
22R-OH Chol	0.02 ± 0.01	0.020 ± 0.003	0.15 ± 0.01	29 ± 3	$5.2 \pm 0.5 \times 10^3$	0.044 ± 0.001
20R,22R-(OH) ₂ Chol	0.03 ± 0.02	0.04 ± 0.01	0.23 ± 0.02	36 ± 7	$6.4 \pm 1.2 \times 10^3$	0.39 ± 0.01
20R,22S-(OH) ₂ Chol	0.12 ± 0.03	0.09 ± 0.02	0.083 ± 0.003	15 ± 2	$5.5 \pm 0.8 \times 10^3$	0.40 ± 0.01
Pregnenolone	0.48 ± 0.22	0.56 ± 0.12	N/A	N/A	N/A	0.55 ± 0.01

All kinetic parameters were calculated from experimental measurements. k_{cat} is the rate of conversion of the corresponding sterol to pregnenolone by P450 11A1. Enzymatic efficiency is reported as k_{cat}/K_m (specificity constant). Abbreviation: Chol, cholesterol.

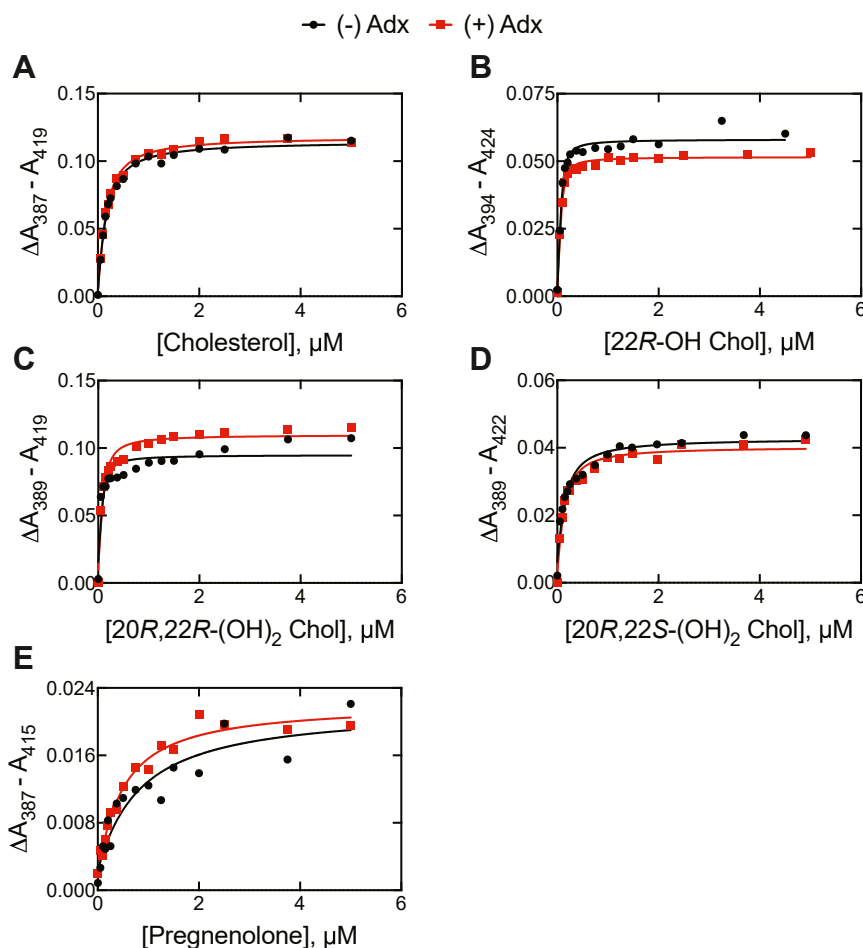


Figure 6. Spectrally-determined K_d values of P450 11A1-steroid complexes. Measurements were made with 0.10 μM P450 11A1 in a 10 cm cuvette both minus (\bullet , black) or in the presence of (0.10 μM) Adx (\blacksquare , red). The titration curves are shown in the insets. Chol: cholesterol. A, cholesterol: K_d 0.12 \pm 0.01 μM without Adx, 0.11 \pm 0.01 μM with Adx. B, 22R-OH cholesterol: K_d 0.02 \pm 0.01 μM without Adx, 0.020 \pm 0.003 μM with Adx. C, 20R,22R-(OH)₂ cholesterol: K_d 0.03 \pm 0.02 μM without Adx, 0.04 \pm 0.01 μM with Adx. D, 20R,22S-(OH)₂ cholesterol: K_d 0.12 \pm 0.03 μM without Adx, 0.09 \pm 0.02 μM with Adx; E, pregnenolone: K_d 0.48 \pm 0.22 μM without Adx, 0.56 \pm 0.12 μM with Adx. See Table 1. Each data point corresponds to one measurement in singlet. Adx, adrenodoxin; P450, cytochrome P450.

Binding of Adx to P450 11A1 \pm cholesterol

Because Adx has been reported to stimulate the binding of P450 11A1 to its substrates (12, 44), we examined whether the binding of detergent-free P450 11A1 to Adx is enhanced by cholesterol, utilizing our fluorescently-labeled Adx construct

(Alexa 488-Adx) (45). A 1:1 M complex of P450 11A1 and cholesterol was gradually titrated into a solution containing Alexa 488-Adx (50 nM), and the quenching of Adx fluorescence was monitored over the course of the reaction. We found that cholesterol stimulated (\sim 4.5-fold) the binding of

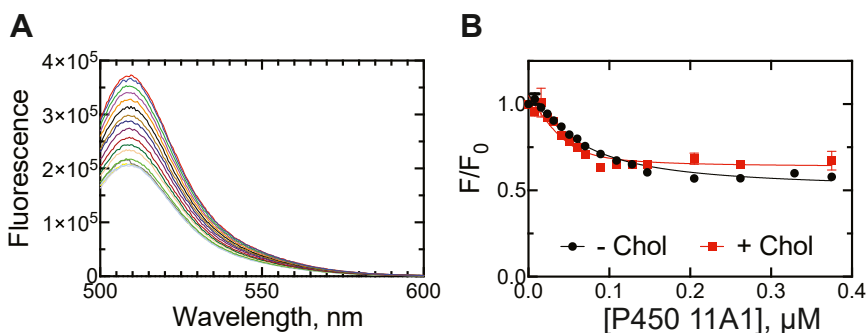


Figure 7. Effect of cholesterol on P450 11A1 binding to Adx. A, titration of P450 11A1 (0–400 nM) into Alexa 488-Adx (50 nM) gradually quenched the fluorophore and yielded a decrease in fluorescence output (between 500 and 600 nm). Spectra were collected after each addition of P450. B, normalized fluorescence (F/F_0) of titrations of P450 11A1 with (\blacksquare , red) and without (\bullet , black) cholesterol (equimolar). A 1:1 M complex of P450 and cholesterol was used as titrant, where indicated. Data were fit to a quadratic equation. Adx, adrenodoxin; P450, cytochrome P450.

Processivity of P450 11A1

P450 11A1 to Adx, as observed by a moderate reduction in the dissociation constant (K_d) from 38 [CI 29–49] nM (without sterol) to 8.2 [CI 3.7–16] nM (with sterol) (Fig 7). We note that these values are similar to the K_d values of 24 nM (without sterol) and 8.2 nM (with sterol) reported by Yablokov *et al.* (46) for human P450 11A1 and the value of 13.4 nM (without sterol) reported by Schiffler *et al.* (47) for bovine P450 11A1, both using surface plasmon resonance methods.

Steroid k_{off} rate measurements

Ketoconazole is a broad spectrum P450 inhibitor that is known to bind tightly to P450 11A1 (48). Interaction of the azole nitrogen atom with the P450 heme produces a bathochromic (“type II”) spectral shift (to ~ 430 nm)—an inverse effect of the binding of substrate. The rapid binding of ketoconazole to unliganded P450 11A1 ($\geq 5 \times 10^5 \text{ M}^{-1} \text{ s}^{-1}$, data not shown) and the low K_d values observed for the studied sterols

afforded the opportunity to use the inhibitor in a “trap” experiment, wherein solutions of aqueous ketoconazole (20 μM) and P450-sterol complex (1:1, 2 μM each) are mixed on a rapid timescale (diluting all reaction components 2-fold). Upon mixing, free enzyme (yielded from the dissociation of the P450-sterol complex) is rapidly captured by aqueous ketoconazole, and the resulting P450-inhibitor complex is detected by the corresponding type II spectral transition. The rate of ketoconazole binding to the free enzyme (k_{on}) is then an estimate for the rate of dissociation of the P450-sterol complex, which we report as k_{off} (Fig. 8).

The k_{off} rate was measured for each sterol in the reaction pathway (Fig. 1). Plots for the cholesterol intermediates (22R-OH and 20R,22R-(OH)₂) were monophasic with k_{off} rates of 0.04 and 0.39 s^{-1} , respectively (Table 1). Higher K_d values for cholesterol and pregnenolone (Fig. 6) yielded biphasic plots in the trap experiment, owing to a greater fraction of unliganded enzyme available at equilibrium. Biexponential fitting of the

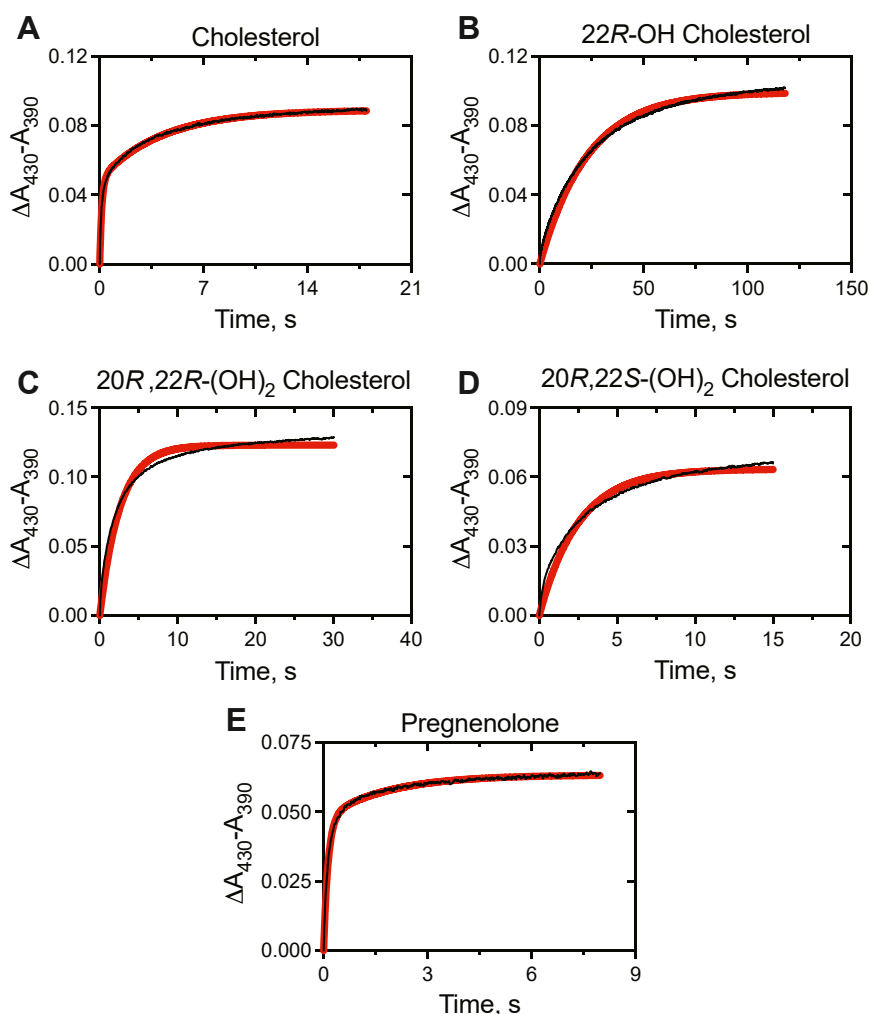


Figure 8. k_{off} measurements of P450 11A1-steroid complexes. In each case, an equimolar concentration of P450 11A1 (2 μM) and each steroid (2 μM), in one syringe, was mixed with a 20 μM concentration of ketoconazole in the other syringe, in an OLIS RSM-1000 stopped-flow spectrophotometer. Full spectra were collected and the A_{390} and A_{430} data were used in the calculations. A, cholesterol: $0.24 \pm 0.01 \text{ s}^{-1}$; (B), 22R-OH cholesterol: $0.044 \pm 0.001 \text{ s}^{-1}$; (C), 20R,22R-(OH)₂ cholesterol: $0.39 \pm 0.01 \text{ s}^{-1}$; (D), 20R,22S-(OH)₂ cholesterol: $0.40 \pm 0.01 \text{ s}^{-1}$; (E), pregnenolone: $0.55 \pm 0.01 \text{ s}^{-1}$. Fits were made to single (B–D) or double (A and E) exponentials using the GraphPad Prism program, following transfer of x, y data files, and the error estimates are also from that program. The red lines show the data traces and the thinner black lines are the fits with the indicated rates. See Table 1. A minimum of eight replicate traces were averaged to yield each plot. P450, cytochrome P450.

cholesterol and pregnenolone data yielded fast phases that were consistent with the ketoconazole k_{on} rate (7.1 and $7.9 \times 10^5 \text{ M}^{-1} \text{ s}^{-1}$, respectively) and slow phases corresponding to dissociation of the P450-sterol complex (k_{off}) prior to ketoconazole trapping (0.24 and 0.55 s^{-1} , respectively). For all the sterols we examined except 22*R*-OH cholesterol, the experimentally determined steady-state forward rate of oxidation was slightly slower than the k_{off} rate. The k_{off} rates were not measured in the presence of Adx as we did not observe an effect of the redox partner when determining ligand dissociation constants (K_{d} , see above).

Measurement of k_{on} rate(s) was not performed because the sterols are delivered in a solution of HPCD, from which the dissociation rate is not known. However, for the purpose of method validation, cholesterol (20 μM in HPCD) was mixed with P450 11A1 and an apparent k_{on} rate of $2.5 \times 10^3 \text{ M}^{-1} \text{ s}^{-1}$ was observed (*i.e.*, 0.05 s^{-1} at 20 μM final concentration), which is >200-fold slower than the k_{on} rate of ketoconazole to unliganded P450 (in the presence of HPCD).

Single turnover kinetics

The reaction of P450 11A1 with cholesterol was followed in a “single-turnover” experiment to measure the rates of formation and disappearance of the oxidized intermediates in the reaction pathway (Fig. 1). As the accumulation of reaction intermediates is characteristic of a distributive reaction, the analysis of intermediate lifetimes is a powerful approach for gauging reaction processivity. In this experiment, enzyme and substrate are preincubated in a 1:1 stoichiometric ratio before reaction initiation—hence “single-turnover.” We have employed the use of rapid quench kinetics to perform this analysis with P450s 2E1, 19A1, 17A1, 11B2, and—most recently—51A1 (30–33, 49).

In this reaction, a 5 μM complex of P450 11A1 and 4.5 μM cholesterol was assembled, and Adx was added at either equimolar (low, 5 μM) or 10-fold excess (high, 50 μM)

concentrations (along with 10 μM AdR). The complex was diluted 2-fold (with 5 mM NADPH) in the apparatus to initiate the reaction, which was quenched at variable times. The products of the reaction were extracted and quantified by radio-HPLC. At low Adx concentrations, the reaction was complete in 3 min with a half-life ($t_{1/2}$) of $\sim 17 \text{ s}$ for the disappearance of cholesterol (Fig. 9A). The reaction was stimulated by excess Adx and was complete in 1 min with a cholesterol $t_{1/2}$ of $\sim 8 \text{ s}$ (Fig. 9B). Reducing the Adx concentration to be equimolar with P450 (*i.e.*, 5 μM) slightly increased (~ 2 -fold) the concentrations of intermediates that accumulated during the reaction (Fig. 9). Overall, however, both reactions rapidly proceeded to final product and no substantial accumulation of intermediate products was observed. (The analysis of kinetic modeling is described below.)

The products of cholesterol oxidation were cleanly resolved with our HPLC separation method, where the order of elution was pregnenolone/20*R*,22*R*-(OH)₂ cholesterol/22*R*-OH cholesterol/cholesterol (Fig. 10). In the single-turnover study with ³H-cholesterol, two peaks were reproducibly seen in the HPLC zone corresponding to 20*R*,22*R*-(OH)₂ cholesterol, at all reaction time points between 0.5 to 5 s (Fig. 10). Both of these radioactive peaks showed similar kinetics of formation and disappearance (Fig. 11). One of these migrated with standard 20*R*,22*R*-(OH)₂ cholesterol, but the possibility was considered that the later eluting peak might be 20*S*,22*R*-(OH)₂ cholesterol (neither eluted with synthetic 20*R*,22*S*-(OH)₂ cholesterol). A mixture of the two ³H-labeled peaks was subjected to treatment with NaIO₄ (which cleaves *vic*-diols), and both peaks disappeared, having converted to pregnenolone (Fig. S14). However, in control experiments without added NaIO₄, the peak with the later t_{R} was converted to the earlier t_{R} peak, that is, 20*R*,22*R*-(OH)₂ cholesterol. This experiment was repeated four times with similar results. We conclude that the two peaks are not diastereomers but are conformers (rotamers) with a $t_{1/2}$ for

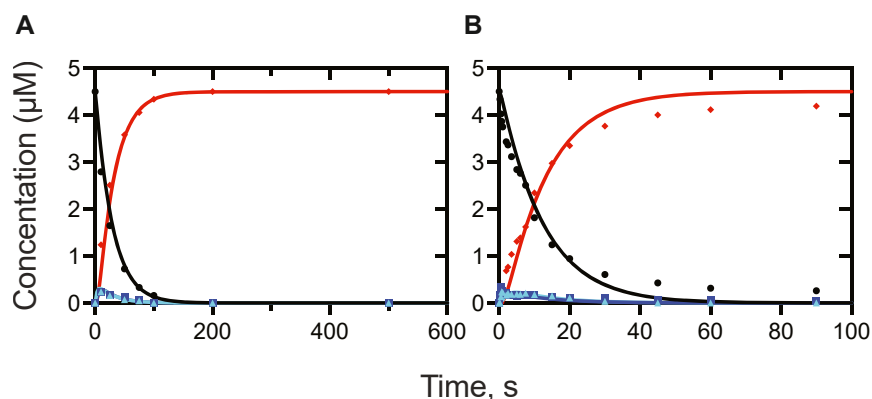


Figure 9. Single-turnover time course of the reaction of a complex of P450 11A1 and [1,2-³H] cholesterol. A, the reaction was initiated by mixing of NADPH (5 mM) from one syringe with a complex of 5 μM P450 11A1, 5 μM Adx, 10 μM AdR, and 4.5 μM [1,2-³H]-cholesterol (HPCD complex) in the other. At each of the indicated times, the reaction was quenched with 1 M HCl and the reaction products were extracted and quantified using radio-HPLC as described in the [Experimental procedures](#). Cholesterol (●—●, black line); 22*R*-OH cholesterol (■—■, dark blue line); 20*R*,22*R*-(OH)₂ cholesterol (▲—▲, light blue line); pregnenolone (◆—◆, red line). Lines are fit to the kinetic mechanism in [Table 2](#) and the indicated rate constants. B, as in Part A, with lines fit to the kinetic mechanism in [Table 2](#) and the indicated rate constants, but with the concentration of Adx in the experiment raised to 50 μM . Each data point is the aggregate of five pooled reactions analyzed as a single sample. AdR, adrenodoxin reductase; Adx, adrenodoxin; HPCD, 2-hydroxypropyl- β -cyclodextrin; P450, cytochrome P450.

Processivity of P450 11A1

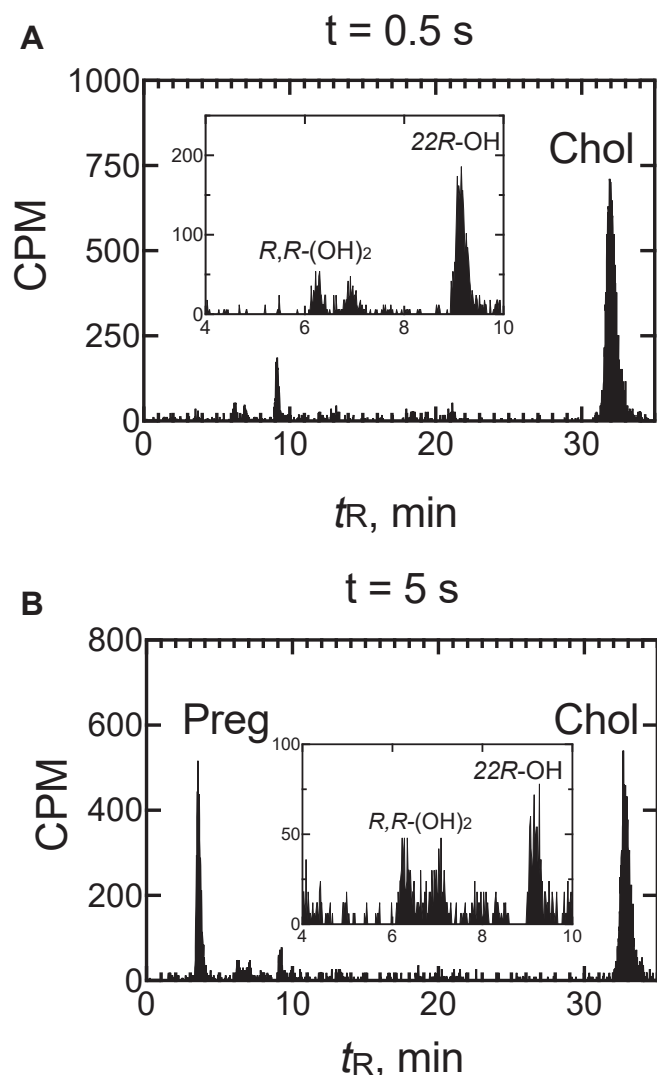


Figure 10. Radio-HPLC of reaction of P450 11A1 with [1,2-³H]-cholesterol under single-turnover conditions and separation of a second dihydroxycholesterol intermediate. Radio-HPLC data from the reaction in Part B of Figure 9. A, chromatogram from HPLC analysis of sample at $t = 0.5$ s; B, chromatogram from HPLC analysis of sample at $t = 5$ s. The insets show the separation of 22R-OH cholesterol (t_R 9.3 min) and the two conformers of 20R,22R-(OH)₂ cholesterol (t_R 6.2 and 6.8 min). P450, cytochrome P450.

conversion on the order of hours for conversion to the more stable form (of 20R,22R-(OH)₂ cholesterol) under our conditions (Fig. 12).

Kinetic isotope effect assays

The results of the single turnover kinetics suggested that the first step of cholesterol oxidation by P450 11A1 is slow and potentially rate-limiting. We synthesized [20, 22, 22]-*d*₃ cholesterol (~32% *d*₃) to investigate whether C-H bond breaking in the first hydroxylation was rate-limiting. P450 11A1 incubations were performed under (low Adx) single-turnover conditions (5 μM P450, 5 μM cholesterol; see [Experimental procedures](#)) with *d*₀- (authentic, unlabeled) and *d*₃-cholesterol, and the disappearance of each was monitored by LC-atmospheric pressure chemical ionization-MS (*m/z*

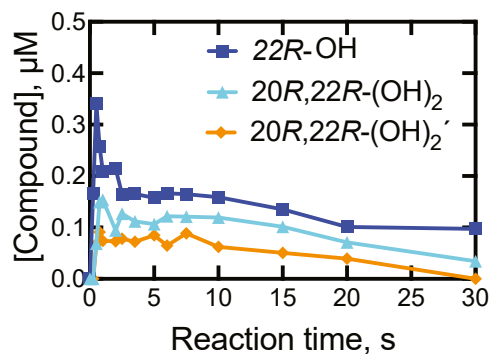


Figure 11. Expansion of the single turnover data from the reaction in Figure 10. A, 22R-OH cholesterol (■—■, dark blue line); 20R,22R-(OH)₂ cholesterol (t_R 6.2 min, Figure 10, ▲—▲, light blue line), and the alternate 20R,22R-(OH)₂ cholesterol conformer (20R,22R-(OH)₂' cholesterol, t_R 6.8 min, Figure 10, ◆—◆, tan line). Each data point is the aggregate of five pooled reactions analyzed as a single sample.

369.3516 and 372.3705, respectively). In theory, if C-H bond breaking were rate-limiting in the initial hydroxylation then the rate of *d*₃-cholesterol consumption would be slower relative to the *d*₀ compound due to the increased strength of a C-D bond. Although the *d* substitution of the cholesterol at C-22 was not complete, the observation of the loss of the *d*₃ isotopologue of cholesterol provides a measurement of the first reaction step under single turnover conditions, in that multiple reaction cycles are not involved.

We did not observe a kinetic isotope effect. Both *d*₀- and *d*₃-cholesterol were oxidized at roughly the same rate, as judged by sterol half-lives ($t_{1/2}$) of 20 s and 22 s, respectively (Fig. 13). A significant ($k_H/k_D \geq 2$) isotope effect would be obvious under our conditions (especially at the earlier time points), based on kinetic simulations in KinTek Explorer (<https://kintekcorp.com/software>). We conclude that C-H bond breaking is not rate-limiting in the 22R-hydroxylation of cholesterol by P450 11A1.

Kinetic modeling

A minimal kinetic model was assembled to fit the data of the single-turnover reactions (Fig. 9) using the parameters listed in Table 2 (Fig. 14). In the model (Figs. S15 and S16), the sterol k_{on} rates (k_1 , k_3 , k_5 , k_7) were set to the experimentally determined value for P450 11A1 and ketoconazole ($5.3 \times 10^5 \text{ M}^{-1} \text{ s}^{-1}$) and sterol k_{off} rates (k_{-1} , k_{-3} , k_{-5} , k_{-7}) were those measured by stopped-flow spectroscopy (Table 1 and Fig. 8). Each oxidation reaction is irreversible, and thus the rates of the reverse reactions (k_{-2} , k_{-4} , k_{-6}) were set to zero. The single-turnover data (Fig. 9) were fit to a single exponential to calculate the first-order decay of cholesterol, that is, the rate of cholesterol 22R-hydroxylation (k_2). This rate (0.09 s^{-1} , when 10-fold (50 μM) excess Adx was used) was comparable to our experimentally determined steady-state k_{cat} of pregnenolone formation from cholesterol (0.12 s^{-1} , Fig. 5A and Table 1). The rate of 20R-hydroxylation of 22R-OH cholesterol (k_4) was estimated similarly to k_2 from exponential fitting of first-order formation of the 20R,22R-(OH)₂ sterol from the 22R-OH sterol. The rate of C-C bond cleavage (k_6) was estimated as the steady-state rate

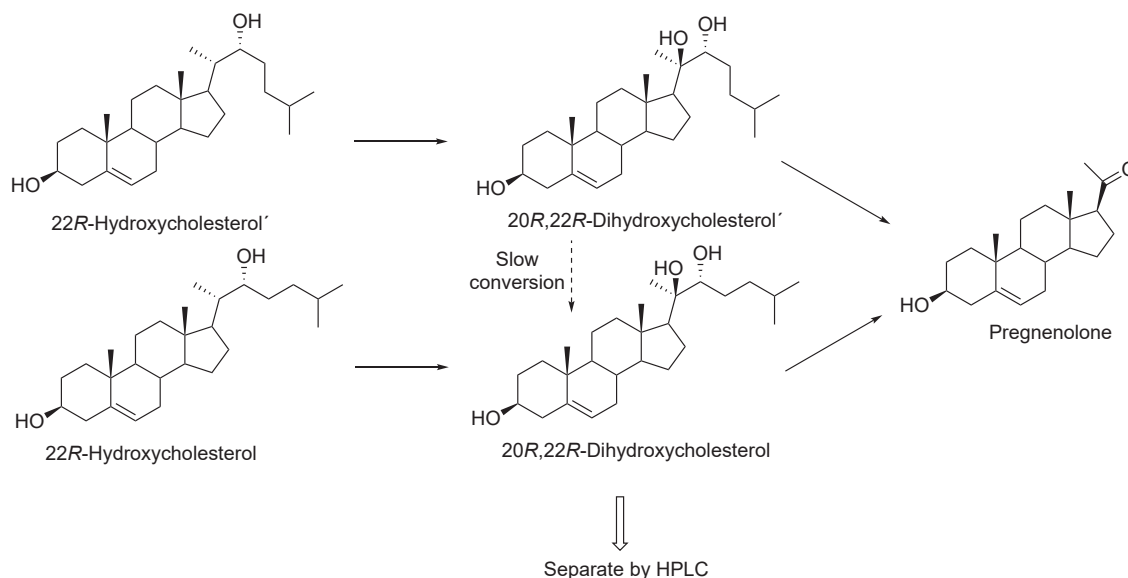


Figure 12. Proposed explanation for 20R-hydroxylation of 22R-OH cholesterol to form rotamers of 20R,22R-(OH)₂ cholesterol. 22R-OH cholesterol' and 20R,22R-(OH)₂ cholesterol' represent less stable conformers of 22R-OH and 20R,22R-(OH)₂ cholesterol, respectively.

determined earlier (Fig. 5C and Table 1). These parameters (k_2 , k_4 , and k_6) were then adjusted by visual approximation to yield the values reported in Table 2 which were used for kinetic modeling as they gave the most satisfactory fits to the experimental data (Figs. 9, S15, and S16). Notably, the rate constants for both hydroxylation of 22R-OH cholesterol and C-C cleavage (Table 2) were much faster (1.5 s^{-1} and 1.7 s^{-1} , respectively) than the steady-state k_{cat} values determined earlier (Fig. 5 and Table 1), attributed to the influence of other steps in the steady-state assays.

Discussion

A procedure was developed to purify human P450 11A1 in the absence of nonionic detergents, in order to avoid many of the previous complications with this enzyme. We used the purified human P450 11A1 to evaluate its properties and the kinetics—and thermodynamics—of several steps in the overall

reaction and to reexamine some earlier reports in the literature. What emerges is a description of the 3-step side chain cleavage reaction in which a rate-limiting initial 22R-hydroxylation is followed by two rapid steps, and the k_{off} rate constants of all the intermediate products/substrates are low.

Much of the early work in the P450 11A1 field was done with the bovine enzyme, isolated from adrenal glands, so strict comparisons may not be possible. Our own measurements were made with recombinant bovine Adx, although our studies with other mitochondrial P450s have not shown any significant differences between bovine and human Adx (37). We were able to develop a method to solubilize recombinant human P450 11A1 with the ionic detergent CHAPS and then remove it by dialysis without the addition of Tween 20 or other nonionic detergents. The protein remained soluble and was catalytically active.

Tween 20 was strongly inhibitory to activity (Fig. 3). Our k_{cat} value for conversion of cholesterol to pregnenolone was $6.9 \text{ nmol product formed min}^{-1} (\text{nmol P450})^{-1}$ (at 40-fold excess Adx) (Table 1 and Fig. 5A). Rates in the literature vary at least from 0.29 (17) to an unusually high value of 34 (20) $\text{nmol product min}^{-1} (\text{nmol P450})^{-1}$ with the bovine and human enzymes, with almost all $<10 \text{ min}^{-1}$, utilizing a variety

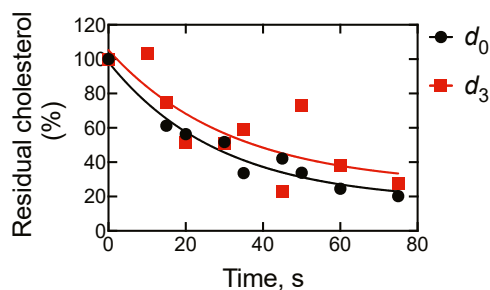


Figure 13. Lack of a kinetic isotope effect in cholesterol 22R-hydroxylation. The disappearance of d_0 -cholesterol (●—●, black line, $5 \mu\text{M}$) and d_3 -cholesterol (◆—◆, red line, $5 \mu\text{M}$) is plotted against reaction time. The disappearance of substrate is normalized to the 0 s control reactions with P450 11A1 ($5 \mu\text{M}$). Both plots were fit to nonlinear (exponential decay) regression models for comparison. The rates observed in this experiment with d_0 - and d_3 -cholesterol were 0.035 and 0.032 s^{-1} , respectively. Incubations were run in singlet and rates were calculated and plotted. P450, cytochrome P450.

Table 2
Model and rate constants used in single turnover kinetic modeling

Reaction step	Steps	k^+ (low, high Adx)	k^-
$\text{E+S} \leftrightarrow \text{ES}$	k_1, k_{-1}	$5.3 \times 10^5 \text{ M}^{-1} \text{ s}^{-1}$	0.24 s^{-1}
$\text{ES} \rightarrow \text{EP}$	k_2, k_{-2}	0.04, 0.12 s^{-1}	0
$\text{E+P} \leftrightarrow \text{EP}$	k_3, k_{-3}	$5.3 \times 10^5 \text{ M}^{-1} \text{ s}^{-1}$	0.044 s^{-1}
$\text{EP} \rightarrow \text{EQ}$	k_4, k_{-4}	0.4, 1.5 s^{-1}	0
$\text{E+Q} \leftrightarrow \text{EQ}$	k_5, k_{-5}	$5.3 \times 10^5 \text{ M}^{-1} \text{ s}^{-1}$	0.39 s^{-1}
$\text{EQ} \rightarrow \text{ER}$	k_6, k_{-6}	0.55, 1.7 s^{-1}	0
$\text{E+R} \leftrightarrow \text{ER}$	k_7, k_{-7}	$5.3 \times 10^5 \text{ M}^{-1} \text{ s}^{-1}$	0.55 s^{-1}

E: P450 11A1, S: cholesterol; P: 22R-OH cholesterol; Q: 20R,22R-(OH)₂ cholesterol; R: pregnenolone. k^+ : k_{on} , k^- : k_{off} .

Processivity of P450 11A1

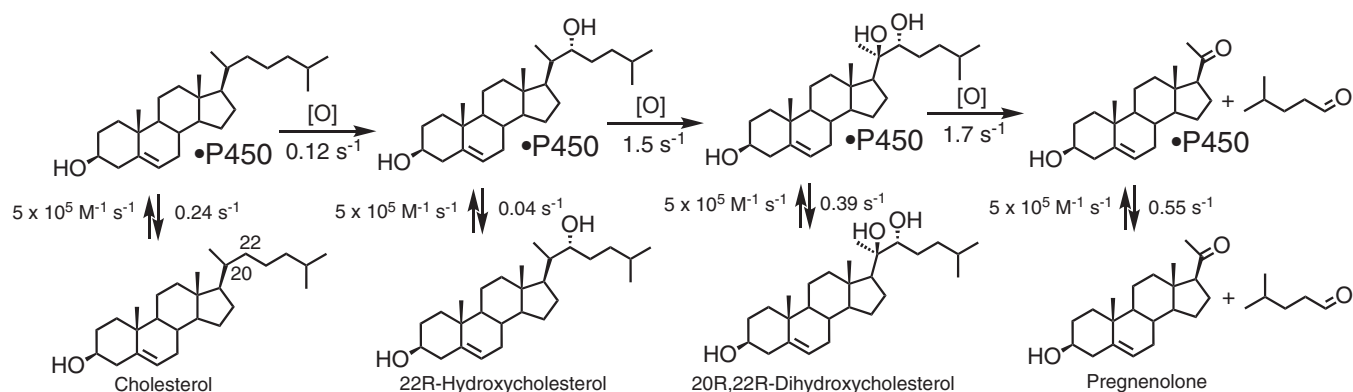


Figure 14. Three-step oxidation of cholesterol to pregnenolone by P450 11A1 and estimated rate constants for individual steps. The same rate constant was used for binding of all ligands to P450 11A1 ($5 \times 10^5 \text{ M}^{-1} \text{ s}^{-1}$). See Table 2 and Figs. S15 and S16. P450, cytochrome P450.

of other assay methods. Although much has been published about roles of specific lipids and phospholipids with P450 11A1 enzymes (12, 38, 39, 44), we observed no stimulation of activity by these under our conditions (Fig. 4). In fact, cardiolipin—a major phospholipid constituent of the mitochondrial inner membrane—was found to inhibit P450 11A1 activity. Although P450 11A1 is a membrane-bound enzyme, the electron carrier Adx is a soluble protein, and the assumption should not be made that P450 11A1 requires a lipid environment (at least when the substrates are delivered in cyclodextrins). This may be true in general for mitochondrial P450s; *e.g.*, with P450 27C1 we did not observe any effect of L- α -dilauroyl-*sn*-glycero-3-phosphocholine on initial rates (50). We have not compared K_m values in the literature, but these are only useful when coupled to k_{cat} , that is, using the ratio k_{cat}/K_m as a specificity constant (51).

Although reports have appeared that the presence of Adx enhances the affinity of P450 11A1 for its substrates by 10- to 20-fold (12, 44), we did not see this effect when we examined P450 11A1-Adx complexes (Fig. 6). (The K_d for a P450 11A1-Adx complex is low (Fig. 7), so most of these two proteins were complexed in these titrations (Fig. 6).) If the binding of cholesterol to P450 11A1 is not enhanced by Adx, then (using a “thermodynamic box” analysis (44, 52, 53)) the binding of cholesterol to P450 11A1 should not have a dramatic effect on the binding of Adx to P450 11A1, which was indeed the case in an assay using Adx tagged with a fluorescent dye, that is, a 4.5-fold change, which translates into $<1 \text{ kcal mol}^{-1}$ change in Gibbs free energy ($\Delta\Delta G = -RT \ln(K_{d,1}/K_{d,2})$) (54) (Fig. 7). This observation is supported by Yablokov *et al.* (46), who found that the K_d of a (human) P450 11A1-Adx complex decreased from 24 nM to 8.2 nM (utilizing surface plasmon resonance) when cholesterol was added to the experiment, reporting very similar values to ours and constituting a roughly ~ 3 -fold decrease in K_d in the presence of cholesterol. Strushkevich *et al.* (7) similarly failed to observe a role of Adx in sterol binding to human P450 11A1, reporting no difference in binding affinities of P450 11A1-Adx fusion proteins for either cholesterol or the 22R-OH intermediate compared to the native enzyme (in the absence of Adx). These results can be contrasted with a study with the bovine enzyme,

however, in which a 30-fold enhancement was reported using a different approach (44).

All of the hydroxy sterols, as well as cholesterol and pregnenolone, produced low-to high-spin changes that could be used to monitor spectral binding and to measure rates of release from P450 11A1. Lambeth *et al.* (53) reported that 22R-OH cholesterol caused a low-spin shift, but this conclusion is presumably due to the weaker spectral shift relative to other ligands (Fig. 6B). Previously reported K_d values for P450 11A1 ligands vary considerably (26, 27). We used a 10-cm spectrophotometer cell to lower the enzyme concentration for these assays, reducing the P450 11A1 concentration to 100 nM (Fig. 6), and applied quadratic fitting because of the low K_d values, which were as low as ~ 20 nM (for 22R-OH cholesterol) (Fig. 6). Many of the values reported in the literature (with bovine P450 11A1) are considerably higher (27). The previous (bovine P450 11A1) values most similar to ours are actually those of Orme-Johnson *et al.* (26) (4.9 nM for 22R-OH cholesterol and 81 nM for 20R,22R-(OH)₂ cholesterol), which is surprising in that these were obtained using equilibrium dialysis, a method not generally well-suited to highly insoluble ligands. It has been reported that the binding of the intermediate hydroxy sterols is 100- to 300-fold tighter than for cholesterol (12), but this difference was considerably less in our work (Table 1 and Fig. 6).

It was also reported (with the bovine enzyme (12)) that the association and dissociation of both cholesterol and 20R,22R-(OH)₂ cholesterol were both complete within the dead time of a stopped-flow instrument, that is, $k > 300 \text{ s}^{-1}$, but our dissociation rates are clearly much slower (Fig. 8). (because of the use of HPCD, we did not estimate binding (“on”) rates for the sterols, in that these likely reflect the dissociation from the cyclodextrin, at least in part.)

Some articles have reported the absence of hydroxy cholesterol intermediates between cholesterol and pregnenolone in P450 11A1 reactions (14, 16) but others have observed one or two (21, 23, 24). Sugano *et al.* (21) did only with a low concentration of Adx. Mast *et al.* (55) reported the presence of 22R-OH cholesterol in the bovine eye (retina and also pigment epithelium), which seems unusual in light of our work, but the possibility exists that another P450 (or a non-P450 oxidase)

performs only this single hydroxylation. We detected intermediates in single turnover experiments, starting with cholesterol (Figs. 9 and 11). The levels of the intermediates were similar with 1:1 and 10:1 M ratios of Adx to P450 11A1 (Fig. 9). This result seems to contrast with that seen by Sugano *et al.* (21) for 20R,22R-(OH)₂ cholesterol. The results could be fit to a model with high processivity, that is, a high ratio of the rate of each oxidation state to the product dissociation rate (Fig. 14). (The oxidation rate of C-C cleavage extracted from kinetic modeling (Fig. 14) is considerably faster than the value determined in the steady-state, which we attribute to a hereto unknown rate-limiting step.)

During analysis of the single turnover experiments, we detected a second radioactive peak (derived from cholesterol) with a retention time (t_R) in the region of 20R,22R-(OH)₂ cholesterol, that is, preceding both 22R- and 22S-OH cholesterol (Fig. 10). The amount of radioactivity in that peak was similar to that in the peak that migrated with standard 20R,22R-(OH)₂ cholesterol. It did not migrate with standard 20R,22S-(OH)₂ cholesterol. Radioactivity eluted with 22R-OH cholesterol, but not 22S-OH cholesterol (Fig. 10). It would be highly unlikely for the stereochemistry to change at the C-22 carbon in the course of the second hydroxylation (at C-20). The peak corresponding to the unknown was collected and treated with sodium periodate (NaIO₄), after which all of the radioactivity migrated with pregnenolone. The result confirms that the unknown compound is a vicinal glycol, that is, a 20,22-(OH)₂ cholesterol.

Based on the kinetic results with 20R,22R-(OH)₂ cholesterol, we propose that P450 11A1 binds 22R-OH cholesterol in two forms (Fig. 12), which we do not really know the shapes of. Each form can be hydroxylated (*via* hydrogen abstraction at C-20) to give the corresponding conformer of 20R,22R-(OH)₂ cholesterol. The two conformers of 20R,22R-(OH)₂ cholesterol were formed at similar rates and were further oxidized (to cleave the side chain) at similar rates (Fig. 11). The two 20R,22R-(OH)₂ cholesterol conformers are apparently stable to acid and to CH₂Cl₂ extraction (see [Experimental procedures](#)) and are separable by HPLC (Fig. 10), which is not unusual for rotamers (*e.g.*, formamidopyrimidine nucleic acids) (56, 57). Upon standing, however, one conformer (t_R 6.8 min, Fig. 11) converts to the more stable one (t_R 6.2 min in Fig. 10). To our knowledge, the formation of multiple, separable conformers has not been observed previously in P450 reactions.

The observation that multiple conformers of 20R,22R-(OH)₂ cholesterol are intermediates in the reaction sequence complicates proposals about the mechanism of the C-C bond cleavage. We have proposed that this last step involves the reaction of compound I (FeO³⁺) with either the C-20 or C-22 OH (10) (¹⁸O label (from ¹⁸O₂) was neither incorporated into pregnenolone nor the enzymatic byproduct, 4-methylpentanal), either of which may be possible, as is a theoretical proposal involving proton abstraction and selective transfer from the C-22 hydroxyl (11). A theoretical study (11) concluding a proton-coupled electron transfer mechanism is consistent with the ¹⁸O₂-labeling results (10). However, the calculations in the

theoretical paper (11) are based on crystal structures with either 22R-OH (6, 58) or 22S-OH cholesterol (58) or the synthetic 20R,22R isomer of (OH)₂ cholesterol (58), which has generally been accepted to be the intermediate (15). However, the enzyme showed similar specificity constants for 20R,22R- and 20R,22S-(OH)₂ cholesterol (Fig. 5). Most importantly, not only was 20R,22R-(OH)₂ cholesterol identified as an intermediate in the single-turnover studies (Fig. 5) but what we identified as a conformer of the 20R,22R-isomer also was, and the rates of formation and cleavage were similar in the presteady-state work (Figs. 9 and 10). (Morisaki *et al.* (15) had also shown that other isomers—20S,22S and 20S,22R—could act as substrates of the enzyme, albeit being less efficient.) Accordingly, any mechanistic conclusions based on only the more stable 20R,22R-(OH)₂ conformer are subject to caveats about interatomic distances, and so on.

In conclusion, our results indicate that P450 11A1 is not inherently dependent upon a lipid environment for catalytic activity and that the nonionic detergent Tween 20 inhibits the enzyme. The 3-step, 6-electron oxidation is a highly processive process due to the relatively low off-rates of the intermediates and the rapid oxidation of 22R-OH cholesterol and 20R,22R-(OH)₂ cholesterol. We report an alternate and significant intermediate in the process, a conformer that arises from an alternate enzyme-substrate conformation in the second hydroxylation step of the reaction. The first hydroxylation (conversion of cholesterol to 22R-OH cholesterol) is rate-limiting in the overall sequence (Table 2 and Fig. 9). However, C-H bond breaking does not appear to be rate-limiting within that step (Fig. 13). The rate-limiting step within the reactions remains unknown; Schiffler *et al.* (47) reported that the rate of reduction of the bovine P450 11A1 by Adx is much faster than the oxidations (30–50 s⁻¹), though the possibility that reduction of the human enzyme by its redox partner is slower cannot be excluded.

Experimental procedures

Chemicals

Cholesterol and pregnenolone were purchased from Millipore-Sigma-Aldrich and used without further purification. [1,2-³H]-Cholesterol was from American Radiolabeled Chemicals. 22R- and 22S-OH cholesterol were purchased from Steraloids. Dansylhydrazine was from Millipore-Sigma-Aldrich and used without further purification.

Chemical synthesis

See [Supporting information](#) section for 20R,22R-(OH)₂ cholesterol, 20R,22S-(OH)₂ cholesterol, [20,22,22-²H₃]-cholesterol (*d*₃-cholesterol), and 4-methylpentanal.

Preparation of steroid-HPCD solutions

Sterol solutions were prepared by adding dry powders directly to HPCD solution (45%, w/v). Mixtures were sonicated, heated (37 °C), and mixed with a vortex device until fully dissolved. When necessary, incubation was performed overnight with shaking (37 °C, 200 rpm) to ensure full

Processivity of P450 11A1

incorporation into the cyclodextrin. Sterol solutions were stored at 4 °C and were heated and sonicated prior to use.

Enzymes

Adx (59) and AdR (60) were expressed in *Escherichia coli* and purified as described previously. The expression and purification of P450 11A1 has been modified from previous procedures (3) and is described below.

Expression of P450 11A1

A P450 11A1 gene insert with a C-terminal His₆ tag (codon-optimized) was digested and gel purified out of pCWori+ using the restriction enzymes NdeI and HindIII before being ligated into pET23C(+) (digested with the same enzymes) according to standard protocols. The P450 11A1 plasmid was transformed into *E. coli* C41(DE3) cells along with molecular chaperones GroES/GroEL according to standard heat shock procedures. An aliquot of the transformation was plated on LB agar supplemented with ampicillin and chloramphenicol and allowed to incubate (37 °C) overnight. A single colony was used to inoculate LB broth (100 ml) supplemented with ampicillin (100 µg ml⁻¹) and chloramphenicol (20 µg ml⁻¹). This preculture was incubated overnight with shaking (37 °C, 250 rpm). Bulk cultures (1 l, in 2.8-L Fernbach flasks) were prepared from terrific broth media supplemented with antibiotics (equivalent to the LB media) and arabinose (4 mg ml⁻¹, for GroES/GroEL induction) and were inoculated with preculture (10 ml). Bulk cultures were grown (37 °C, 250 rpm, ~3 h) until the OD₆₀₀ reached ~0.4 to 0.6, at which point P450 expression was induced by the addition of isopropyl β-D-1-thiogalactopyranoside (1 mM) and δ-aminolevulinic acid (1 mM) and flasks were supplemented with fresh ampicillin (50 µg/ml). Induced cultures were incubated (28 °C, 95 rpm, ~48 h) until harvest by centrifugation (3500g, 30 min, 4 °C). Pellets were stored at -80 °C until use.

Purification of P450 11A1

Cell pellets were thawed on ice and gradually resuspended in a sonication buffer (100 ml per cell pellet (obtained from a one-liter culture)) composed of potassium phosphate buffer (100 mM, pH 7.4) containing glycerol (20%, v/v), Mg(C₂H₃O₂)₂ (6 mM), DTT (0.1 mM), and one cOmplete EDTA-free Protease Inhibitor Cocktail tablet (Roche) per 50 ml resuspension. Cells were lysed by sonication on ice in a 600 ml stainless steel beaker using a Model FB505 (500 W) probe instrument (Thermo Fisher Scientific) equipped with a bolt tip for 15 min (15 s on/45 s off, 45% intensity). The lysate was centrifuged (14,500g, 50 min, 4 °C) to remove debris and the supernatant was subjected to ultracentrifugation (10⁴g, 60 min, 4 °C) to collect membranes. Pellets were gently resuspended in a buffer composed of potassium phosphate buffer (100 mM, pH 7.4) containing glycerol (20%, v/v), EDTA (0.1 mM), 2-mercaptoethanol (10 mM), and sodium CHAPS (1%, w/v) and the resuspension was stirred (resolubilized) overnight (4 °C). The solution was again subjected to ultracentrifugation and the supernatant was applied to a metal

affinity (Ni-nitrilo triacetate) column (1.5 cm × 8 cm, ~15 ml) previously equilibrated with equilibration buffer (potassium phosphate buffer (100 mM, pH 7.4) containing glycerol (20%, v/v), NaCl (500 mM), and imidazole (20 mM)). The column was washed with equilibration buffer (10 column volumes), after which the concentration of imidazole in the buffer was increased to 50 mM (3 column volumes), 80 mM (3 column volumes), and finally 100 mM (3 column volumes) before elution of P450 with 150 mM imidazole (3 column volumes). The P450 band (red) began to migrate during the 100 mM wash and was fully displaced during the 150 mM elution. Column fractions were pooled based on absorbance (417 nm), concentrated with centrifugal concentrators (30 kDa molecular weight cut-off (to <10 ml), and dialyzed against a buffer of potassium phosphate buffer (200 mM, pH 7.4) containing glycerol (20%, v/v), and DTT (0.1 mM) using dialysis tubing (6–10 kDa molecular weight cut-off). P450 11A1 (<10 ml) was dialyzed against four volumes (1 l) of buffer, yielding a final maximal imidazole concentration <2 nM (Figs. S11 and S12). The material (20.3 µM) was aliquoted and stored at -80 °C until use.

UV-visible spectroscopy

Spectra were recorded using either an OLIS-Cary 14 or OLIS-Aminco DW2a instrument (On-Line Instrument Systems) in the split-beam mode. The OLIS-Cary 14 instrument was used in the P450 11A1 titrations with a 10-cm cell (Starna Cells, catalog no. 34-Q-100, volume 25 ml).

Binding of Alexa 488-Adx to P450 11A1

A previously described Alexa Fluor 488-labeled Adx construct and experimental protocol were used (45) to perform the fluorescence titration of P450 11A1 with Adx. Alexa 488-Adx (50 nM) was prepared in potassium phosphate buffer (100 mM, pH 7.4) in a 1 ml glass cuvette. P450 11A1 was gradually titrated (0–0.4 µM) into the cuvette (to a maximum of 2% (v/v)), and spectra were recorded using an OLIS DM-45 spectrofluorometer (1.24 mm slit width) with fluorophore excitation at 493 nm and scanning emission spectra from 500 to 600 nm. To investigate whether cholesterol affects the binding of Adx to P450 11A1, we performed the titrations with and without cholesterol. A 1:1 stoichiometric ratio of P450 11A1 and cholesterol (20 µM) was performed and titrated into the cuvette. *K*_d values were calculated fitting plots of the normalized fluorescence at emission maximum *versus* concentration of P450 11A1 using a quadratic equation in GraphPad Prism.

LC-MS assays of conversion of steroids to pregnenolone

Steady-state kinetic assays were performed with a P450:AdR:Adx molar ratio of 1:2:40, and preliminary experiments established optimal conditions for P450 11A1 activity. Reactions were performed by reconstituting P450 (0.25 µM), AdR (0.5 µM), and Adx (10 µM) on ice for 10 min prior to dilution in potassium Hepes buffer (50 mM, pH 7.4) and H₂O and the addition of substrate (sterol, in HPCD (45% w/v)).

Sterol dilutions were performed in HPCD to ensure that the HPCD composition was equal throughout all incubations (final 4.5% w/v). The reaction mixture was split between vials (425 μ l in each), and reactions were preincubated (37 $^{\circ}$ C, 5 min) prior to initiation (75 μ l) with an NADPH-generating system (0.5 mM NADP⁺, 10 mM glucose 6-phosphate, and 2 μ g ml⁻¹ glucose 6-phosphate dehydrogenase) (61). Reactions (5 min) were terminated by extraction into CH₂Cl₂ (2 ml) and transferred to an ice bath. After the experiment was complete, the quenched reactions were subjected to centrifugation (10³g, 5 min, 23 $^{\circ}$ C) to separate layers, the organic (bottom) layer of each sample was removed (1.6 ml) to fresh glass vials, and the samples were brought to dryness under a stream of nitrogen.

Steroid extracts were subsequently derivatized with dansylhydrazine and analyzed as described previously (42). Briefly, the dried residue was resuspended (200 μ l) in C₂H₅OH (fortified with 0.1% v/v CF₃CO₂H, as the derivatization reaction is H⁺-catalyzed) and mixed with a vortex device. Samples were transferred to 1.5 ml amber glass vials, solutions of dansylhydrazine (10 mM) and DHEA, 10 μ M, as internal standard) were added, and vials were capped, mixed with a vortex device, and incubated in the dark overnight (~16 h, 23 $^{\circ}$ C). The derivatization reaction was quenched with acetone (50 mM), briefly incubated in the dark (~30 min, 23 $^{\circ}$ C), and was then neutralized with base (250 μ l of 0.5 M NaOH) and extracted into CH₂Cl₂ (1 ml). The samples were mixed with a vortex device and the organic (bottom) layer was removed (0.8 ml) to clean amber vials. Solvent was again removed under nitrogen, and the dried residue was dissolved in a mobile phase (100 μ l) of 0.1% CF₃CO₂H in aqueous CH₃CN (50%, v/v) for analysis.

Samples were injected (10 μ l, held at 25 $^{\circ}$ C) on a 2.1 mm \times 50 mm (1.7 μ m) Acquity BEH octadecylsilane (C₁₈) column (held at 40 $^{\circ}$ C) using a Waters Acquity UPLC with a flow rate of 0.2 ml min⁻¹ and a gradient mobile phase of (A) 0.1% aqueous HCO₂H and (B) CH₃CN as follows (all %B, v/v): 0 min, 40%; 0.5 min, 40%; 8 min, 100%; 8.5 min, 95%; 9 min, 100%; 9.1 min, 40%; and 10 min, 40%. The column eluate was subjected to electrospray ionization (beginning at *t*_R 3.5 min to avoid the acetone dansyl hydrazone) and the product (pregnenolone dansyl hydrazone) was detected using a Waters QDa on-line mass spectrometer (Waters) set in the positive-ion electrospray mode using a cone voltage of 15 V, a sampling frequency of 10 Hz, and scanning from *m/z* 150 to 800. Data were processed using MassLynx software (Waters). Standard curves (of pregnenolone, with DHEA as internal standard) were prepared fresh for each assay, and product formation was assessed relative to the quotient of pregnenolone and DHEA peak areas.

***K_d* determination**

K_d values were determined by difference spectroscopy as previously reported (33, 43) but with some modifications. Briefly, a long-path quartz cuvette (10 cm, 25 ml) containing P450 11A1 (0.1 μ M, in 100 mM potassium phosphate buffer (pH 7.4)) was prepared and a baseline was recorded in an OLIS-Cary 14 spectrophotometer. Where indicated, the redox

partner Adx was added in equimolar concentration (0.1 μ M) to P450. Sterol solutions (in 45% HPCD, w/v) were added to the cuvette, the contents of the cuvette were inverted to mix, and a spectrum was recorded (350–500 nm) after each addition. The total volume added to each cuvette was kept \leq 2% (v/v, 0.25 ml) in the assay. The maximum absorbance difference (usually $\Delta A_{390}-A_{418}$) was plotted against the total sterol concentration, and the data were fit to a quadratic equation in GraphPad Prism software (GraphPad, <https://www.graphpad.com>) to estimate the dissociation constant (*K_d*). A quadratic equation was used to correct the ligand concentration for the enzyme-bound concentration (used as $Y = B + \frac{A}{2} * \frac{1}{E} * ((Kd+E+X) - \sqrt{(Kd+E+X)^2 - (4 * E * X)})$ (or $Y = B + (A/2)*(1/E)*((Kd + E + X) - \sqrt{(Kd + E + X)^2 - (4*E*X)})$ in Prism software), where E = enzyme concentration, *K_d* = dissociation constant, and X = free sterol concentration).

Single-turnover kinetics

Low Adx concentration (benchtop)

P450 11A1 (5 μ M) was reconstituted with its redox partners AdR (10 μ M) and Adx (5 μ M) on ice (10 min) prior to dilution in potassium Hepes buffer (50 mM, pH 7.4) and H₂O and the addition of ³H-cholesterol substrate (4.5 μ M, 0.5 Ci/mmol). The concentration of substrate was deliberately kept slightly below the enzyme concentration to ensure that single-turnover conditions were strictly followed. The mixture (0.75 ml) was preincubated (37 $^{\circ}$ C, 5 min) in a shaking water bath prior to initiation with an equal volume of NADPH solution (5 mM, from a 10 mM stock in 50 mM potassium Hepes buffer, pH 7.4), thus reducing the concentrations of all enzymes and substrate to one-half their starting concentrations. After completing the desired incubation time, an aliquot (200 μ l) was removed from the incubation and added to vials containing aqueous HCl (800 μ l, 1 M). The quenched reactions were mixed with a vortex device and placed on ice. When the time course was complete, the quenched reactions were mixed with CH₂Cl₂ (5 ml) to extract reaction products and were centrifuged (10³g, 5 min, 23 $^{\circ}$ C) to separate layers, and the organic (bottom) layers were transferred (4 ml) to fresh glass vials. The extraction process was repeated and the two extracts (2 \times 4 ml) from each sample were combined to maximize product recovery. Samples (8 ml) were brought to dryness under a stream of nitrogen, and the dried residues were dissolved in CH₃OH (75 μ l) and transferred to autosampler vials for analysis by radio-HPLC.

High Adx concentration (rapid quench)

Enzyme and NADPH solutions were prepared as described for the benchtop experiments (above) but with the modification that the concentration of Adx was increased to 50 μ M (from 5 μ M). Due to the stimulation of P450 11A1 cholesterol side-chain cleavage activity by high concentrations of Adx (Fig. 2), this reaction had to be monitored at sub-second intervals that were achievable with the use of a rapid quench-flow apparatus (KinTek). The rapid quench-flow is a rapid mixing device that combines equal volumes (~19 μ l) of two

Processivity of P450 11A1

solutions (P450 and NADPH, held at 37 °C) into a central internal chamber to initiate a reaction. After the preset reaction time is completed, the mixture (~38 μl) is then rapidly combined with a quench solution (1 M HCl, ~160 μl), expelled from the apparatus, and collected in vials. Utilizing this experimental design, the reaction of enzyme-substrate complex (P450 11A1-Adx-AdR and ^3H -cholesterol) was initiated with NADPH on a variable timescale (0–90 s), pooling five replicates of each time point to maximize sensitivity. The products of each quenched reaction (~1 ml) were extracted with two volumes (5 ml) of CH_2Cl_2 , brought to dryness, and dissolved in CH_3OH as described for the benchtop experiments.

Radio-HPLC conditions

Samples (held at 4 °C) were injected (50 μl) using a Agilent 1100 Series HPLC system on a NovaPak (Waters) octadecylsilane (C_{18}) 3.9 mm \times 100 mm (4 μm) column (held at 25 °C) with a flow rate of 1.0 ml min^{-1} using a gradient mobile phase of (A) H_2O and (B) CH_3CN as follows (all in % B, v/v): 0 min, 70%; 10 min, 100%; 35.5 min, 100%; 37 min, 30%; and 40 min, 70%. The flow rate was increased to 1.5 ml min^{-1} (from the 10 min to 10.5 min interval) to decrease the retention of cholesterol and was later returned to 1.0 ml min^{-1} (from the 35 min to 35.5 min interval) to prepare for the next injection. The column eluate was mixed (1:2, v/v) with Flow-Logic U scintillation cocktail (LabLogic) and radioactivity (^3H) was detected using a β -RAM Model 5 radioflow detector (IN/US, LabLogic). Analytes were quantitated on the basis of their ^3H peak areas relative to the summed radioactivity of the four compounds of interest.

Kinetic isotope effect

The kinetic isotope experiment was designed similarly to the benchtop experiment described above, but with some modifications. P450 11A1 (5 μM) was reconstituted with the redox partners AdR (10 μM) and Adx (5 μM) on ice (10 min) prior to dilution in potassium Hepes (50 mM, pH 7.4) and H_2O and addition of d_3 -cholesterol substrate (5 μM). The mixture was preincubated (5 min) prior to initiation with NADPH (2.5 mM, from 25 mM in potassium Hepes (50 mM, pH 7.4)) thus bringing all components to their desired final concentrations. After completing the desired incubation time, an aliquot (500 μl) was removed from the incubation and added to vials containing CH_2Cl_2 (5 ml) and the vials were mixed with a vortex device and placed on ice. The quenched reactions were centrifuged (10³g, 5 min, 23 °C) to separate layers, and the organic (bottom) layers were removed (4 ml) and transferred to fresh glass vials. The extraction process was repeated and the two extracts (2 \times 4 ml) from each sample were combined to maximize product recovery. Samples (8 ml) were brought to dryness under a stream of nitrogen, and the dried residues were dissolved in CH_3OH (25 μl) and transferred to autosampler vials for analysis.

Samples (held at 4 °C) were injected (10 μl) using a Waters Acquity UPLC system on a Acquity BEH octadecylsilane (C_{18})

2.1 mm \times 50 mm (1.7 μm) UPLC column (held at 25 °C) with a flow rate of 0.5 ml min^{-1} using an isocratic mobile phase of CH_3CN (only). The column eluate was subjected to atmospheric pressure chemical ionization and analyzed using a Thermo Fisher Scientific LTQ XL Orbitrap mass spectrometer instrument operating in positive mode, scanning from m/z 100 to 500, with a resolution setting of 120,000. Data were processed using Xcalibur QualBrowser (Thermo Fisher Scientific) software (version 2.0.7; <https://www.thermofishcer.com/order/catalog/product/OPTON>).

k_{off} determination

Determinations of k_{off} rates were performed as previously described (33). Briefly, an OLIS-RSM 1000 stopped-flow spectrophotometer (held at 23 °C) with slit widths of 1.24 mm (8 nm bandpass) and scanning from 350 to 500 nm was loaded with solutions of (A) ketoconazole (20 μM , in 100 mM potassium phosphate buffer (pH 7.4)) and (B) P450 11A1 (2 μM , same buffer). These solutions were mixed (in equal volumes, giving a two-fold dilution of all reaction components), and the observed rate of ketoconazole binding (ΔA_{430}) to P450 was 5.3 s^{-1} . Then, sterol (in HPCD) was added in equimolar concentration (2 μM) to P450 11A1 and the mixture was loaded into the drive syringe and mixed with solution A (ketoconazole). The rate of ketoconazole binding is given by $\Delta A_{430} - A_{390}$ (displacement of sterol (decrease in A_{390}) due to ketoconazole binding (increase in A_{430})) and is an estimate for the rate at which the P450-sterol complex dissociated (k_{off}).

NaIO_4 treatment of diols

The treatment of vicinal glycols with NaIO_4 was performed *via* modification of a procedure reported by Ho *et al.* (62). P450 11A1 was incubated (0.5 s) with ^3H -cholesterol according to the single-turnover (high Adx) conditions described above. The products of the reaction (extracted, dried, and dissolved in CH_3OH (75 μl)) were injected (45 μl) for analysis by radio-HPLC as described and the diol region (t_{R} 5.8 min to 7.3 min, Fig. 10) was collected into vials. The diols (in ~1:9 $\text{H}_2\text{O}:\text{CH}_3\text{CN}$ (v/v, ~2 ml)) were extracted into CH_2Cl_2 (5 ml), the bottom layer (4 ml) was removed to a fresh vial, and the extraction process was repeated twice to maximize product recovery. The extracts (3 \times 4 ml) were pooled and brought to dryness under a stream of nitrogen gas, and the dried residue was dissolved in CH_3OH (100 μl). The diol sample was split (2 \times 50 μl) between autosampler vials and one sample was treated with aqueous NaIO_4 (2.5 mg ml^{-1}) while the other was treated with H_2O . Preliminary experiments with 20R,22R- and 20R,22S-(OH)₂ cholesterol established that NaIO_4 incubations were optimal with heating (37 °C) and that the reaction of the 20R,22S-(OH)₂ cholesterol required substantially longer to go to completion (~24 h) than did the natural substrate 20R,22R-(OH)₂ (~3 h). Accordingly, all NaIO_4 incubations were performed at 37 °C for 24 h. After completion of the reaction, the samples were injected (20 μl) on radio-HPLC (Fig. S14) using the conditions described earlier.

Kinetic modeling

Data were imported into KinTek Explorer software (v. 11.01, KinTek, <https://kintekcorp.com/software>) (63) as txt files and processed using an Apple computer (operating system 11.6.2). The indicated kinetic model (Table 2) was used with the enzyme and substrate concentrations, first estimating the rate of disappearance of the substrate cholesterol. Further adjustment of the individual rate constants was done to obtain the best fit, and the rate constants are reported (Figs. S15 and S16).

Data availability

All data are available in the Supporting information in the form of synthetic procedures and characterization of chemicals, plus NMR, mass, and UV spectra. Also, key txt files include the data used for calculations for k_{cat} , K_m , and K_d determinations and fitting to kinetic models.

Supporting information—This article contains supporting information (10, 21, 61).

Acknowledgments—We thank Dr Kwangho Kim for technical advice and the use of equipment and reagents in some of the chemical syntheses. We also thank K. Trisler for assistance in preparation of the manuscript.

Author contributions—K. D. M., L. L., and F. P. G. methodology; K. D. M., L. L., Y. T., H. L. W.-S., and F. P. G. validation; K. D. M., L. L., and F. P. G. formal analysis; K. D. M., L. L., Y. T., H. L. W.-S., and F. P. G. investigation; K. D. M., L. L., Y. T., and F. P. G. writing—original draft; K. D. M., and F. P. G. writing—review and editing; K. D. M., L. L., Y. T., and H. L. W.-S., visualization; K. D. M., and F. P. G. supervision; F. P. G. funding acquisition; F. P. G. conceptualization; F. P. G. project administration.

Funding and additional information—This work was supported by grants from the National Institute of General Medical Sciences of the National Institutes of Health (NIH) grant number R01 GM118122 [to F. P. G.]. The content is solely the responsibility of the authors and does not necessarily represent the official views of the NIH. This material is also based upon work supported by the National Science Foundation Graduate Research Fellowship Program under Grant No. 1937963 (K. D. M.). Any opinions, findings, and conclusions or recommendations expressed in this material are those of the author(s) and do not necessarily reflect the views of the National Science Foundation.

Conflict of interest—All of the authors declare that they have no conflict of interest with the contents of this article.

Abbreviations—The abbreviations used are: AdR, adrenodoxin reductase; Adx, adrenodoxin; DHEA, dehydroepiandrosterone; HPCD, 2-hydroxypropyl- β -cyclodextrin; MS, mass spectrometry; P450 (or CYP), cytochrome P450; UPLC, ultra-performance liquid chromatography.

References

- Miller, W. L., and Auchus, R. J. (2011) The molecular biology, biochemistry, and physiology of human steroidogenesis and its disorders. *Endocrin. Rev.* **32**, 81–151
- Tuckey, R. C., Nguyen, M. N., Chen, J., Slominski, A. T., Baldisseri, D. M., Tieu, E. W., *et al.* (2012) Human cytochrome P450_{scc} (CYP11A1) catalyzes epoxide formation with ergosterol. *Drug Metab. Dispos.* **40**, 436–444
- Acimovic, J., Goyal, S., Kosir, R., Golicnik, M., Perse, M., Belic, A., *et al.* (2016) Cytochrome P450 metabolism of the post-lanosterol intermediates explains enigmas of cholesterol synthesis. *Sci. Rep.* **6**, 28462
- Slominski, A. T., Li, W., Kim, T.-K., Semak, I., Wang, J., Zjawiony, J. K., *et al.* (2015) Novel activities of CYP11A1 and their potential physiological significance. *J. Steroid Biochem. Mol. Biol.* **151**, 25–37
- Zhang, D., Flint, O., Wang, L., Gupta, A., Westhouse, R. A., Zhao, W., *et al.* (2012) Cytochrome P450 11A1 bioactivation of a kinase inhibitor in rats: use of radioprofiling, modulation of metabolism, and adrenocortical cell lines to evaluate adrenal toxicity. *Chem. Res. Toxicol.* **25**, 556–571
- Mast, N., Annalora, A. J., Lodowski, D. T., Palczewski, K., Stout, C. D., and Pikuleva, I. A. (2011) Structural basis for three-step sequential catalysis by the cholesterol side chain cleavage enzyme CYP11A1. *J. Biol. Chem.* **286**, 5607–5613
- Strushkevich, N., MacKenzie, F., Cherkesova, T., Grabovec, I., Usanov, S., and Park, H. W. (2011) Structural basis for pregnenolone biosynthesis by the mitochondrial monooxygenase system. *Proc. Natl. Acad. Sci. U. S. A.* **108**, 10139–10143
- Davydov, R., Gilep, A. A., Strushkevich, N. V., Usanov, S. A., and Hoffman, B. M. (2012) Compound I is the reactive intermediate in the first monooxygenation step during conversion of cholesterol to pregnenolone by cytochrome P450_{scc}: EPR/ENDOR/Cryoreduction/Annealing studies. *J. Am. Chem. Soc.* **134**, 17149–17156
- Davydov, R., Strushkevich, N., Smil, D., Yantsevich, A., Gilep, A., Usanov, S., *et al.* (2015) Evidence that compound I is the active species in both the hydroxylase and lyase steps by which P450_{scc} converts cholesterol to pregnenolone: EPR/ENDOR/Cryoreduction/Annealing studies. *Biochemistry* **54**, 7089–7097
- Yoshimoto, F. K., Jung, I. J., Goyal, S., Gonzalez, E., and Guengerich, F. P. (2016) Isotope-labeling studies support the electrophilic compound I iron active species, FeO(3+), for the carbon-carbon bond cleavage reaction of the cholesterol side-chain cleavage enzyme, cytochrome P450 11A1. *J. Am. Chem. Soc.* **138**, 12124–12141
- Su, H., Wang, B., and Shaik, S. (2019) Quantum-mechanical/molecular-mechanical studies of CYP11A1-catalyzed biosynthesis of pregnenolone from cholesterol reveal a C-C bond cleavage reaction that occurs by a compound I-mediated electron transfer. *J. Am. Chem. Soc.* **141**, 20079–20088
- Lambeth, J. D., Kitchen, S. E., Farooqui, A. A., Tuckey, R., and Kamin, H. (1982) Cytochrome P-450_{scc}-substrate interactions: studies of binding and catalytic activity using hydroxycholesterols. *J. Biol. Chem.* **257**, 1876–1884
- Teicher, B. A., Koizumi, N., Koreeda, M., Shikita, M., and Talalay, P. (1978) Biosynthesis of pregnenolone from cholesterol by mitochondrial enzymes of bovine adrenal cortex. The question of the participation of the 20(22)-olefins and 20, 22-epoxides of cholesterol. *Eur. J. Biochem.* **91**, 11–19
- Simpson, E. R., and Boyd, G. S. (1967) The cholesterol side-chain cleavage system of bovine adrenal cortex. *Eur. J. Biochem.* **2**, 275–285
- Morisaki, M., Sato, S., Ikekawa, N., and Shikita, M. (1976) Stereochemical specificity at carbon-20 and -22 of hydroxylated cholesterol for side-chain cleavage by adrenocortical cytochrome P-450_{scc}. *FEBS Lett.* **72**, 337–340
- Heo, G. Y., Liao, W. L., Turko, I. V., and Pikuleva, I. A. (2012) Features of the retinal environment which affect the activities and product profile of cholesterol-metabolizing cytochromes P450 CYP27A1 and CYP11A1. *Arch. Biochem. Biophys.* **518**, 119–126
- Morisaki, M., Duque, C., Ikekawa, N., and Shikita, M. (1980) Substrate specificity of adrenocortical cytochrome P-450_{scc}-I. Effect of structural modification of cholesterol side-chain on pregnenolone production. *J. Steroid Biochem.* **13**, 545–550
- Pikuleva, I. A., Mackman, R. L., Kagawa, N., Waterman, M. R., and Ortiz de Montellano, P. R. (1995) Active-site topology of bovine cholesterol side-chain cleavage cytochrome P450 (P450_{scc}) and evidence for interaction of tyrosine 94 with the side chain of cholesterol. *Arch. Biochem. Biophys.* **322**, 189–197

19. Hartz, P., Strohmaier, S. J., El-Gayar, B. M., Abdulmughni, A., Hutter, M. C., Hannemann, F., *et al.* (2021) Resurrection and characterization of ancestral CYP11A1 enzymes. *FEBS J.* **288**, 6510–6527
20. Tuckey, R. C., and Cameron, K. J. (1993) Side-chain specificities of human and bovine cytochromes P-450_{sc}. *Eur. J. Biochem.* **217**, 209–215
21. Sugano, S., Miura, R., and Morishima, N. (1996) Identification of intermediates in the conversion of cholesterol to pregnenolone with a reconstituted cytochrome P-450_{sc} system: accumulation of the intermediate modulated by the adrenodoxin level. *J. Biochem.* **120**, 780–787
22. Lieberman, S., and Lin, Y. Y. (2001) Reflections on sterol sidechain cleavage process catalyzed by cytochrome P450_{sc}. *J. Steroid Biochem. Mol. Biol.* **78**, 1–14
23. Burstein, S., and Gut, M. (1976) Intermediates in the conversion of cholesterol to pregnenolone: kinetics and mechanism. *Steroids* **28**, 115–131
24. Hume, R., Kelly, R. W., Taylor, P. L., and Boyd, G. S. (1984) The catalytic cycle of cytochrome P-450_{sc} and intermediates in the conversion of cholesterol to pregnenolone. *Eur. J. Biochem.* **140**, 583–591
25. Tuckey, R. C., and Cameron, K. J. (1993) Human placental cholesterol side-chain cleavage: enzymatic synthesis of (22R)-20 α ,22-dihydroxycholesterol. *Steroids* **58**, 230–233
26. Orme-Johnson, N. R., Light, D. R., White-Stevens, R. W., and Orme-Johnson, W. H. (1979) Steroid binding properties of beef adrenal cortical cytochrome P-450 which catalyzes the conversion of cholesterol into pregnenolone. *J. Biol. Chem.* **254**, 2103–2111
27. Jefcoate, C. R. (1975) Cytochrome P-450 of adrenal mitochondria. Spin states as detected by difference spectroscopy. *J. Biol. Chem.* **250**, 4663–4670
28. Fersht, A. (1999) *Structure and Mechanism in Protein Science*, Freeman, New York, NY
29. Guengerich, F. P., Wilkey, C. J., Glass, S. M., and Reddish, M. J. (2019) Conformational selection dominates binding of steroids to human cytochrome P450 17A1. *J. Biol. Chem.* **294**, 10028–10041
30. Sohl, C. D., and Guengerich, F. P. (2010) Kinetic analysis of the three-step steroid aromatase reaction of human cytochrome P450 19A1. *J. Biol. Chem.* **285**, 17734–17743
31. Gonzalez, E., and Guengerich, F. P. (2017) Kinetic processivity of the two-step oxidations of progesterone and pregnenolone to androgens by human cytochrome P450 17A1. *J. Biol. Chem.* **292**, 13168–13185
32. Reddish, M. J., and Guengerich, F. P. (2019) Human cytochrome P450 11B2 produces aldosterone by a processive mechanism due to the lactol form of the intermediate 18-hydroxycorticosterone. *J. Biol. Chem.* **294**, 12975–12991
33. McCarty, K. D., Sullivan, M. E., Tateishi, Y., Hargrove, T. Y., Lepesheva, G. I., and Guengerich, F. P. (2023) Processive kinetics in the three-step lanosterol 14 α -demethylation reaction catalyzed by human cytochrome P450 51A1. *J. Biol. Chem.* **299**, 104841
34. Hosea, N. A., and Guengerich, F. P. (1998) Oxidation of nonionic detergents by cytochrome P450 enzymes. *Arch. Biochem. Biophys.* **353**, 365–373
35. Garewal, H. S. (1973) A procedure for the estimation of microgram quantities of Triton X-100. *Anal. Biochem.* **54**, 319–324
36. De Caprio, J., Yun, J., and Javitt, N. B. (1992) Bile acid and sterol solubilization in 2-hydroxypropyl-beta-cyclodextrin. *J. Lipid Res.* **33**, 441–443
37. Child, S. A., Reddish, M. J., Glass, S. M., Goldfarb, M. H., Barckhausen, I. R., and Guengerich, F. P. (2020) Functional interactions of adrenodoxin with several human mitochondrial cytochrome P450 enzymes. *Arch. Biochem. Biophys.* **694**, 108596
38. Lambeth, J. D., Kamin, H., and Seybert, D. W. (1980) Phosphatidylcholine vesicle reconstituted cytochrome P-450_{sc}: role of the membrane in control of activity and spin state of the cytochrome. *J. Biol. Chem.* **255**, 8282–8288
39. Seybert, D. W., Lancaster, J. R., Jr., Lambeth, J. D., and Kamin, H. (1979) Participation of the membrane in the side chain cleavage of cholesterol. Reconstitution of cytochrome P-450_{sc} into phospholipid vesicles. *J. Biol. Chem.* **254**, 12088–12098
40. Tuckey, R. C., Nguyen, M. N., and Slominski, A. (2008) Kinetics of vitamin D3 metabolism by cytochrome P450_{sc} (CYP11A1) in phospholipid vesicles and cyclodextrin. *Int. J. Biochem. Cell Biol.* **40**, 2619–2626
41. Guengerich, F. P., McCarty, K. D., Chapman, J. G., and Tateishi, Y. (2021) Stepwise binding of inhibitors to human cytochrome P450 17A1 and rapid kinetics of inhibition of androgen biosynthesis. *J. Biol. Chem.* **297**, 100969
42. Guengerich, F. P., Tateishi, Y., McCarty, K. D., and Liu, L. (2023) Steroid 17 α -hydroxylase/17,20-lyase (cytochrome P450 17A1). *Methods Enzymol.* **689**, 39–63
43. Schenkman, J. B., Remmer, H., and Estabrook, R. W. (1967) Spectral studies of drug interaction with hepatic microsomal cytochrome P-450. *Mol. Pharmacol.* **3**, 113–123
44. Lambeth, J. D., Seybert, D. W., and Kamin, H. (1980) Phospholipid vesicle-reconstituted cytochrome P-450_{sc}. Mutually facilitated binding of cholesterol and adrenodoxin. *J. Biol. Chem.* **255**, 138–143
45. Glass, S. M., Webb, S. N., and Guengerich, F. P. (2021) Binding of cytochrome P450 27C1, a retinoid desaturase, to its accessory protein adrenodoxin. *Arch. Biochem. Biophys.* **714**, 109076
46. Yablokov, E. O., Sushko, T. A., Kaluzhskiy, L. A., Kavaleuski, A. A., Mezentsev, Y. V., Ershov, P. V., *et al.* (2021) Substrate-induced modulation of protein-protein interactions within human mitochondrial cytochrome P450-dependent system. *J. Steroid Biochem. Mol. Biol.* **208**, 105793
47. Schiffler, B., Zöllner, A., and Bernhardt, R. (2004) Stripping down the mitochondrial cholesterol hydroxylase system, a kinetics study. *J. Biol. Chem.* **279**, 34269–34276
48. Mast, N., Linger, M., and Pikuleva, I. A. (2013) Inhibition and stimulation of activity of purified recombinant CYP11A1 by therapeutic agents. *Mol. Cell. Endocrinol.* **371**, 100–106
49. Bell, L. C., and Guengerich, F. P. (1997) Oxidation kinetics of ethanol by human cytochrome P450 2E1. Rate-limiting product release accounts for effects of isotopic hydrogen substitution and cytochrome b5 on steady-state kinetics. *J. Biol. Chem.* **272**, 29643–29651
50. Johnson, K. M., Phan, T. T. N., Albertolle, M. E., and Guengerich, F. P. (2017) Human mitochondrial cytochrome P450 27C1 is localized in skin and preferentially desaturates trans-retinol to 3,4-dehydroretinol. *J. Biol. Chem.* **292**, 13672–13687
51. Johnson, K. A. (2019) New standards for collecting and fitting steady state kinetic data. *Beilstein J. Org. Chem.* **15**, 16–29
52. Kyte, J. (1995) *Mechanism in Protein Chemistry*, 1st Ed, Garland, New York, NY
53. Heyl, B. L., Tyrrell, D. J., and Lambeth, J. D. (1986) Cytochrome P-450_{sc}-substrate interactions: role of the 3 β - and side chain hydroxyls in binding to oxidized and reduced forms of the enzyme. *J. Biol. Chem.* **261**, 2743–2749
54. Daniels, F., and Alberty, R. A. (1966) *Physical Chemistry*, 3rd Ed, John Wiley & Sons, Inc., New York, NY
55. Mast, N., Reem, R., Bederman, I., Huang, S., DiPatre, P. L., Bjorkhem, I., *et al.* (2011) Cholestenic acid is an important elimination product of cholesterol in the retina: comparison of retinal cholesterol metabolism with that in the brain. *Invest. Ophthalmol. Vis. Sci.* **52**, 594–603
56. Humphreys, W. G., and Guengerich, F. P. (1991) Structure of formamidopyrimidine adducts as determined by NMR using specifically 15N-labeled guanosine. *Chem. Res. Toxicol.* **4**, 632–636
57. Brown, K. L., Deng, J. Z., Iyer, R. S., Iyer, L. G., Voehler, M. W., Stone, M. P., *et al.* (2006) Unraveling the aflatoxin-FAPY conundrum: structural basis for differential replicative processing of isomeric forms of the formamidopyrimidine-type DNA adduct of aflatoxin B1. *J. Am. Chem. Soc.* **128**, 15188–15199
58. Strushkevich, N., Usanov, S. A., and Park, H. W. (2010) Structural basis of human CYP51 inhibition by antifungal azoles. *J. Mol. Biol.* **397**, 1067–1078

59. Palin, M. F., Berthiaume, L., Lehoux, J. G., Waterman, M. R., and Sygusch, J. (1992) Direct expression of mature bovine adrenodoxin in *Escherichia coli*. *Arch. Biochem. Biophys.* **295**, 126–131
60. Sagara, Y., Wada, A., Takata, Y., Waterman, M. R., Sekimizu, K., and Horiuchi, T. (1993) Direct expression of adrenodoxin reductase in *Escherichia coli* and the functional characterization. *Biol. Pharm. Bull.* **16**, 627–630
61. Guengerich, F. P. (2014) Analysis and characterization of enzymes and nucleic acids relevant to toxicology. In: Hayes, A. W., Kruger, C. L., eds. *Hayes' Principles and Methods of Toxicology*, 6th Ed, CRC Press-Taylor & Francis, Boca Raton, FL: 1905–1964
62. Ho, T. M., Arman, H. D., and Yoshimoto, F. K. (2023) Synthesis of hyocholic acid and its derivatization with sodium periodate to distinguish it from cholic acid by mass spectrometry. *Steroids* **197**, 109260
63. Johnson, K. A., Simpson, Z. B., and Blom, T. (2009) Global Kinetic Explorer: a new computer program for dynamic simulation and fitting of kinetic data. *Anal. Biochem.* **387**, 20–29